SECURITY CLASSIFICATION OF THIS PAGE (When Data Entered)

REPORT DOCUMENTATION PAGE		READ INSTRUCTIONS BEFORE COMPLETING FORM
1. REPORT NUMBER NRL Memorandum Report 5215	2. GOVT ACCESSION NO.	3. RECIPIENT'S CATALOG NUMBER
4. TITLE (and Subtitle) ANALOG FIBER OPTICS: PRAGMATIC CONSIDERATIONS BEYOND THE TEXTBOOK		5. TYPE OF REPORT & PERIOD COVERED Interim report on a continuing NRL problem. 6. PERFORMING ORG. REPORT NUMBER
7. AUTHOR(s) E.L. Althouse, D.M. Kopp and R.G. Trgina		8. CONTRACT OR GRANT NUMBER(s)
9. PERFORMING ORGANIZATION NAME AND ADDRESS Naval Research Laboratory Washington, DC 20375		10. PROGRAM ELEMENT, PROJECT, TASK AREA & WORK UNIT NUMBERS 62721N; XF21222100; 75-0138-0-3
11. CONTROLLING OFFICE NAME AND ADDRESS		12. REPORT DATE December 29, 1983 13. NUMBER OF PAGES 62
14. MONITORING AGENCY NAME & ADDRESS(if different from Controlling Office)		15. SECURITY CLASS. (of this report) UNCLASSIFIED 15a. DECLASSIFICATION/DOWNGRADING SCHEDULE

16. DISTRIBUTION STATEMENT (of this Report)

Approved for public release; distribution unlimited.

17. DISTRIBUTION STATEMENT (of the abstract entered in Block 20, if different from Report)

18. SUPPLEMENTARY NOTES

19. KEY WORDS (Continue on reverse side if necessary and identify by block number)

Fiber-optics
Lasers
Leds

20. ABSTRACT (Continue on reverse side if necessary and identify by block number)

This report discusses the use of AlGaAs lasers and LEDs as optical sources for a multimode fiber-optic link that uses analog modulation. It is well known that the limited linearity of these sources makes digital modulation a preferable method to send information. However, many factors determine how a portion of an information transfer system is constructed or retrofitted including previous investments in

(Continues)

DD FORM 1 JAN 73 1473 EDITION OF 1 NOV 65 IS OBSOLETE
S/N 0102-014-6601

SECURITY CLASSIFICATION OF THIS PAGE (When Data Entered)

20. ABSTRACT (Continued)

associated electrical and electro-optical hardware, the cost of redesigning the system architecture, and, in some instances, the difficulty in digitizing certain modulation waveforms. This report is written primarily for the fiber-optic design engineer that uses analog modulation, for whatever justification, but many aspects will also be of use for those who design with the traditional digital approach.

Based on the LEDs we have tested, third-order linear dynamic ranges up to 75 dB and second-order linear dynamic ranges up to 59 dB have been observed in 3 kHz noise bandwidth at frequencies up to 20 MHz. For links with substantial loss or for frequencies much greater than 20 MHz the performance will be degraded.

For the lasers tested, third-order linear dynamic ranges up to 68 dB and second-order linear dynamic ranges in the vicinity of 50 to 55 dB have been observed in 3 kHz bandwidth at a modulation frequency of 70 MHz. Measurements at 400 MHz indicated a third-order linear dynamic range of 59 dB. Link lengths were typically 500 to 600 meters, but some measurements with a short link indicate that laser performance degrades for link lengths of several hundred meters because of reflections into the laser cavity from distributed regions of the fiber.

Factors that affect fiber-optic system performance are discussed. These include electro-optical transfer characteristics, average power level, modulation sensitivity, device risetime, fiber dispersion, excess microbending loss, excess noise and distortion mechanisms for lasers, temperature effects, and lifetime, particularly with respect to an EMP environment. Techniques to make the best use of available linear dynamic range are discussed. These include using an intermediate FM carrier, using optical rather than electrical summing of FDM carriers, and hard-limiting of angle modulated carriers (followed by bandpass filtering) prior to introduction to the optical link.

NRL Memorandum Report 5215

Analog Fiber Optics: Pragmatic Considerations Beyond the Textbook

E. L. ALTHOUSE, D. M. KOPP AND R. G. TRGINA

Transmission Technology Branch
Information Technology Division

December 29, 1983

NAVAL RESEARCH LABORATORY
Washington, D.C.

CONTENTS

ANALOG FIBER OPTICS: PRAGMATIC CONSIDERATIONS BEYOND THE TEXTBOOK

INTRODUCTION

The basic objective for this report is to present information that is important for analog fiber-optic link design but is not found in most textbooks. Consequently, concepts such as light propagation in the fiber, optical power budgets, and other routine considerations that are thoroughly reported in many textbooks will not be discussed. We assume that the reader has previously acquired this knowledge. The motivation for this report is to expose physical phenomena and technical subtleties that have confronted nearly five years of our effort to interface a military platform to a towed communication buoy via a fiber-optic tow cable. This objective has resulted in a presentation of somewhat disjointed subject material that we consider to be important and deserving of assemblage into a single document.

Modern fiber-optic communication links are designed almost exclusively for digital modulation of the optical lightwave carrier. This design strategy results partially from the fact that digital transmissions can be regenerated at repeater stations with no degradation to the bit-error-rate (or equivalently, signal-to-noise ratio) and as consequence of the fact that the optical drivers (LEDs and lasers) perform poorly with analog modulation.

The deficient performance of optical sources with analog modulation arises from limitations in available source intensity, limitations in linearity, and in the case of the laser, excessive noise. In view of the shortcomings of optical sources for analog modulation and the obvious advantage of digital modulation, the question "Why use analog modulation?" is frequently posed.

There are probably very few good technical reasons for designing an optical link using analog modulation rather than digital. However, there are situations in which large sums of money have previously been invested in a multichannel communication system that was designed initially with intent of using a conventional electrical transmission line between the sections of a distributed receiving system. Examples of a distributed receiving system include towed communication buoys and acoustic arrays and radio equipped balloons and kites. Typical operational requirements such as high strength, low weight, small size, and (occasionally) multiple power conductors frequently mandate the use of a highly strengthened cable (steel or KEVLAR reinforcement) that has insufficient core space remaining for one or more high performance electrical transmission lines. Because of the small size and high performance of optical fiber transmission lines, the design engineer will naturally explore the potential of fiber-optics to improve the link performance. Because of the large previous investment in analog system development and the prospect of a comparable additional investment in a digital redesign, the engineer may be forced to consider analog transfer on the fiber-optic link unless a simple digital add-on to the existing system is feasible.

Manuscript approved September 2, 1983.

When part of the communication link is formed by electromagnetic or radio-wave transmission, the analog world cannot be entirely avoided. Even "digital" radio transmissions are achieved by some form of modulation of one or more RF carriers. Carrier modulations are achieved by angle modulation (frequency or phase), amplitude modulation (single side band (SSB) for most military users) or in some cases a combination of both (e.g. 16 QAM). Although AM (SSB) modulation has long been recognized to be a poor choice when security and survivability in a military environment are necessary, it is still commonly used in the HF and UHF bands for routine, nonsecure voice transmissions.

Linearity is important in the transmission and processing of the radio wave carriers. The most serious effect of system nonlinearity is the generation of intermodulation products that (can) fall back into the information or processing bandwidth and interfere with the desired signal. The intermodulation products are caused by a nonlinear mixing of two or more carriers of differing frequencies. The presence of multiple carriers could be a consequence of frequency-division-multiplexing (FDM) on a single transmission line (optical or electrical) or a result of an interfering radio wave that is within the RF bandwidth of the receiver.

Although the effect of nonlinearity is most severe for the amplitude modulated signal, angle modulated carriers are also susceptible. The fact that the first step in the detection of angle modulated carriers is hard-limiting does not imply that linearity in the preceding stages is unimportant. An "intermod" produced from the desired angle modulated carrier and an interfering carrier will share some of the modulation characteristics of the desired signal and some of the characteristics of the interfering signal. If the amplitude of the intermod is not negligible and its frequency falls within the processing bandwidth of the detector, the effect will be to add noise to the detection of the zero-crossings. Consequently, whenever fiber-optic components form a part of a radio receiver or constitute a part of a link to a radio receiver, their linearity must be known and must be adequate for the specific application.

Some military communication systems, for which we have a specific interest, necessitate a significant separation between the antenna and the signal processing hardware. The ideal interface between the antenna and the signal processor would be a lossless, wideband RF transmission line (Figure 1) that would require no intermediate electronics and would produce little degradation to the communications. Unfortunately, an electrical transmission line with a length of 0.5 km or greater that would approach the bandwidth and loss requirements at frequencies from VLF through UHF either does not exist or falls short of space and weight restrictions. Furthermore, the concept fails at lower frequencies where size limitations force the antenna to be electrically short and impedance matching between the antenna and transmission line can be achieved only by the addition of electronics between the antenna and transmission line.

With the advent of low-loss, high-bandwidth optical fibers, there have been suggestions to achieve the ideal interface between the signal processor and remotely located antenna by using electro-optics as shown in Figure 2. The basic problem with this system is associated with the goal to achieve

wideband performance. The problem is not with the optical fiber, since it has adequate bandwidth and linearity, but lies instead with insufficient linear dynamic range of the source or source-fiber combination. For any receiving system that is subject to sources of interference, the wider the bandwidth is allowed to be, the greater the linear dynamic range must be to avoid overloading. For the bandwidths that have been previously implied (say tens to hundreds of megahertz), there is probably not an electrical amplifier in existence that would have a sufficient linear dynamic range to provide the required sensitivity without overloading when exposed to sources of moderate to strong interference. Optical sources, such as solid state LEDs and injection lasers, would be even less satisfactory as components of the wideband link because of their inferior linearity.

A practical compromise to the ideal link between the remote antenna and the signal processor is shown in Figure 3. A set of mixers are used to convert a selected radio frequency to a manageable, fixed intermediate frequency which is converted back to the original RF at the end of the link so that a standard receiver can be used without modification. The link bandwidth is equal to that of the IF filter which is usually not more than about ten times the modulation bandwidth. Linear dynamic range requirements for the link components are reduced because of the decrease in the carrier bandwidth. The system can be used over a wide RF range by using a programmable synthesizer as a source for the local oscillator.

Many antenna systems deliver carriers from several different frequency bands simultaneously over a link to a set of receivers using frequency-division multiplexing (FDM) as illustrated in Figure 4. This permits more information to pass over the link while minimizing the linear dynamic range requirements of the link components by keeping the IF bandwidths of each carrier as small as practical. However, an additional source of difficultly for this design approach is the generation of intermodulation products from nonlinear mixing of the carrier frequencies on the link. This problem is reduced by controlling and minimizing the amplitudes of each carrier by exploiting amplitude limiting techniques appropriate to the frequency and modulation of the individual carrier.

A scheme for minimizing carrier amplitudes is shown in Figure 5. The lower frequency radio signals (say the VLF and LF bands) are passed directly through a voltage-to-frequency converter, producing a frequency modulated carrier that is amplitude limited and bandpass filtered. With this conversion scheme the signal-to-noise ratio (SNR) is achieved by frequency excursions, rather than amplitude excursions, and a given SNR can be achieved at a much smaller carrier amplitude than is possible with direct amplitude modulation. The use of an intermediate FM carrier to improve the performance of an analog fiber-optic link is discussed in references [1, 2, 3].

When the frequency of the radio carrier becomes excessive for direct voltage-to-frequency conversion, a frequency converter (mixer) can be used to produce a lower intermediate frequency (IF) that is suitable for voltage-to-frequency conversion. When the incoming radio wave has angle modulation, the carrier can be converted to a manageable IF, hardlimited, bandpass filtered, and passed through the link. At the other end of the link this

signal will be separated from the other FDM carriers, hardlimited again, and then introduced to the remainder of the detection circuitry. The FM channels will be discriminated and mixed back up to the original radio frequency.

The foregoing discussion has been general in that the techniques discussed can be applied to either an optically or electrically transmitted link carrier. When a fiber-optic link is used, the electrical summation of FDM carriers can be replaced by an optical summation as indicated in Figure 6. The advantage to this method is that the optical summation is very linear and mixing products between the FDM carriers will be avoided. The only intermodulation products that will occur are those produced by mixing of the frequency components, contained in the passband of each carrier channel, at the electrical-to-optical conversion. Harmonic products will also be passed through the link; however, a judicious choice of carrier frequencies will often prevent these products from contaminating any bands of interest. The additional link loss introduced by the optical couplers is at least partially counterbalanced by the fact that each optical source can be modulated more intensely per information carrier than is possible when a single optical source is modulated with a composite FDM information carrier.

We have indicated that there is a wide variety of ways in which a fiber-optic antenna-to-receiver link can be designed. The more linearity the link exhibits (linearity is usually limited by the optical source), the wider the carrier bandwidth can be and the fewer the signal-preparatory operations need be. Consequently the designer of such a system must have information regarding the signal-to-noise and distortion characteristics of candidate optical sources in order to make intelligent design decisions. The intent of this report is to provide a sufficient amount of test data for candidate LEDs and lasers to allow appropriate design decisions to be made.

The scope of this report is limited to the 800 to 900 nanometer (nm) wavelength region, which is served by AlGaAs source technology, and to the use of multimode optical fiber. We assume that the reader has a basic understanding of light propagation in optical waveguides.

The remaining sections of this report address issues such as a quantitative measure of linear dynamic range, how digitization of incoming information/waveforms can be used in place of analog processing, the various factors that influence the type of optical source chosen for a particular application, the specific and pertinent attributes of lasers and LEDs, specific measurements of linear dynamic range for lasers and LEDs, and, finally, a summary of the most important issues and facts.

DEFINITION OF LINEAR DYNAMIC RANGE

Having discussed the linearity of electronic and electro-optical components rather loosely to this point, it is necessary to define an understandable and readily observable measure of linearity. We shall equate linear dynamic range (LDR) to what is sometimes called spurious-free dynamic range [4] which is defined in terms of an intercept point (IP) and a noise floor (N_0) for a specific order of distortion.

Figure 7 shows a graphical relationship between the intercept points, the fundamental input/output transfer characteristic, the intermodulation (IM) characteristics, the noise floor, and the LDRs. The intercept point is a technical figure-of-merit that is routinely used by manufactures to specify the distortion characteristics of an electrical component such as a mixer or amplifier. It is obtained by determining the intersection of the linear projection of the fundamental transfer characteristic with the projection of the IM characteristic for a given order of distortion. The key to understanding the relationship is the fundamental requirement that for each 1 dB increase in input power there will be a 3 dB increase in IM_3 and a 2 dB increase in IM_2. For our studies of optical components we have omitted a determination of intercept point but determined the LDRs by plotting fundamental, IM_2, IM_3, and noise data in the manner of Figure 7 and by observing the point at which the signal equals noise (minimum signal) and the point at which IM_2 or IM_3 equals the noise (maximum signal). The difference in dB between these two points defines the LDR for the order of distortion considered.

Considering only second order distortion,

$$LDR_3 = \frac{2}{3} (IP_3 - N_0) \text{ in dB} \qquad (1)$$

where IP_3 is the third-order intercept point and N_0 is the noise floor in a specified bandwidth. Note that if N_0 is proportional to bandwidth, then for every 1 dB reduction in bandwidth, LDR_3 increases by 2/3 dB.

Considering only second order distortion,

$$LDR_2 = 1/2 (IP_2 - N_0) \text{ in dB} \qquad (2)$$

where IP_2 is the second-order intercept point. If N_0 is proportional to bandwidth, then for each 1 dB decrease in bandwidth, LDR_2 increases by 1/2 dB.

For LED and laser sources, the LDR_2 is always smaller than LDR_3. For those systems in which frequency management can keep IM_2 products from falling into bands of interest, the LDR_3 will be the important design parameter. For those systems which will be degraded by the presence of IM_2 components, the LDR_2 will be of dominant importance.

THE DIGITAL ALTERNATIVE

When economics, technological ability, and other practical constraints permit, the link between the remote antenna and the signal processor should employ digital transfer of information. The simplest and most practical approach to digitization is to extract the information from the carrier at the site of the antenna. If the information extracted from the carrier is digital in nature, the electro-optical interface to a fiber-optic link is simple and bit rates less than 3000 per second would be adequate for many communications channels. If the information extracted from the carrier is analog, as for a voice channel, then digital samples would be taken at a

rate at least twice the desired voice bandwidth and with a sufficient number of quantization bits to provide the desired audio fidelity. For telephone systems, toll quality fidelity is achieved at a 64 kbps (PCM) rate. If the channel is used exclusively for voice and never for data, then predictive coding techniques can be used to reduce the bit rate.

There are, however, situations in which the modulation (information) cannot be extracted from the carrier(s) in a simple way. Spread spectrum and frequency hopped signals fall into this category, and although these modulations are not presently in wide use, they are sure to become part of the next generation of military communication systems. Adding to the difficulty of information extraction and digitization at the site of the antenna(s) is that some systems provide a communication service over many bands (VLF through UHF for example) with each band having one or more forms of modulation (SSB, FSK, PSK). Some navigation channels are critically dependent upon a comparison of the time varying phase of the incoming RF carrier to a stable reference frequency. Each information channel will typically have a receiver that shares little commonality with the receiver for another channel. When the antenna platform is a balloon or towed vehicle, it is undesirable to have the total ensemble of receiver hardware collocated with the antenna because of the large expense of the hardware and the short or unpredictable lifetime of the platform.

For those communication/navigation channels for which the receiver hardware cannot be placed at the site of the antenna, the only digital alternative is to sample the channel IF bandwidth (which is usually significantly larger than the detection bandwidth) with sufficient amplitude quantization to permit subsequent recovery by the detector of a weak desired signal in the presence of a strong inband interfering signal. Presently, integrated circuit chips are available that provide 14 (Analog Devices, ADC 131) to 16 (Burr Brown, PCM 75) bit quantization at conversion rates of 83 kHz to 58 kHz. With these devices a 25 kHz bandwidth IF (DC to 25 kHz) could be digitized, transmitted over the link at an approximate 1 Mbps rate and reconstructed with 84 to 96 dB quantized-limited dynamic range. For many systems of interest, this performance would be adequate and may even provide an improvement to the present analog method of carrier transfer when the effects of external pickup and crosstalk on the analog link are fully accounted for.

In spite of the fact that digital transfer of communications over a link may appear feasible and superior to analog transmission, the design engineer is sometimes forced (at least in the short-term) to retain the previously developed system architecture and to provide relatively simple upgrades that do not require major restructuring of the system. When such situations force a consideration of fiber-optic components for an analog relay, the data from this report will provide useful guidance.

FACTORS INFLUENCING THE CHOICE OF OPTICAL SOURCE

Deciding whether the optical source for the analog link should be a laser or an LED requires a careful consideration of the properties of each source and the influence these properties have on the overall system performance. Such an analysis should start at the detector and work back toward the source.

Influence of Average Power on the Detector

The SNR (rms-to-rms) at the output of a non-avalanche (PIN) photodetector may be written as

$$SNR = \frac{(RP_o k/L)^2/2}{[2qRP_o/L + (RP_n/L)^2 + I_t^2]B} \qquad (3)$$

where P_o is the average optical power coupled into the fiber, L is the optical loss of the link (expressed as a ratio), k is the optical modulation index, R is the responsivity of the photodetector in units of Amperes per unit optical power, q is the electron charge (1.6×10^{-19}), I_t is the equivalent thermal noise current of the photodetector in Amperes per root Hertz.

P_n is the excess optical noise density associated with a laser source, and B is the noise bandwidth. The numerator is equal to the square of the rms signal current developed at the detector. The first term on the left side of the denominator is the square of the rms quantum noise current which is proportional to the average power incident on the detector. The middle term in the demoninator is the square of rms current associated with the excess noise of the laser. For simplicity we assume that P_n is independent of L; however, this may not be completely true because a significant part of P_n originates from modal interaction in the fiber, causing the value of P_n to increase as a weak function of L.

The assumption that P_n is independent of L permits a qualitative comparison to be made between the SNRs resulting from the use of a laser and an LED as a function of link loss. To obtain data for the comparison we make additional, reasonable assumptions:

- P_o is ten times larger for the laser than for the LED
- quantum noise ($2qRP_o/L$) is equal to $10I_t^2$ at L = 1 for the laser (= I_t^2 for the LED)
- $(RP_n/L)^2 = 100\ I_t^2$ at L = 1 for the laser (= 0 for the (LED))

The result of applying these assumptions to equation (3) is shown in Figure 8. At very small link loss the performance of the LED is close to that of the laser; however, as the loss increases the laser appears superior (ignoring other considerations such as distortion) because the rate of decrease of the SNR with L (out to at least 12 dB) is much less than for the LED. Consequently, for a given application the optical loss budget will determine which type of source is better assuming all else equal and that the noise characteristics of the laser and photodetector have been determined.

Power in the Fiber

Moving our attention from the detector toward the source we will now consider the properties of the fiber. Of prime importance is the amount of optical power that can be coupled into a low loss fiber having the desired frequency bandwidth. If the emitting area and numerical aperture of the source are larger than those of the fiber there will be considerable coupling loss at the source-fiber junction. Assuming otherwise perfect alignment the loss between elements 1 and 2 is given by [5]

$$L = \frac{A_1 (NA_1)^2}{A_2 (NA_2)^2} \qquad (4)$$

where $A_2 \leq A_1$ and $NA_2 \leq NA_1$

and where the radiation is from element 1 to element 2, the A's are cross-sectional areas, and the NA's are the numerical apertures. In equation (4) the functional dependence on area ratio is exact but the dependence on numerical aperture ratio is an empirical approximation. Equation (4) is applicable to the junction of two dissimilar fibers or to the junction of a source to a fiber. For example, a Motorola MFOE108F LED emits approximately 1.5 mW of optical power at a 100 mA bias into a 0.200 mm optical port with an NA = 0.5. The amount of this power that can be coupled into a fiber with a .050 mm core and an NA = 0.23 is $1500\left(\frac{.050}{.200}\right)^2 \left(\frac{.23}{.5}\right)^2$ = 19.9 microwatts

indicating a coupling loss of 18.8 dB.

If axial, lateral, and angular alignments are not perfect, additional losses will occur. These have been measured and reported in references [6, 7, and 8]. Reflections at the interfaces between media of different refractive indices, n_1 and n_2, will cause a Fresnel loss given by [9]

$$L = 10 \log \left[1 + \left(\frac{n_1 - n_2}{n_1 + n_2} \right)^2 \right] \qquad (5)$$

and result in a loss of about 0.35 dB for a coupling between two silica fibers when an index matching fluid is not used.

The emitting area of most injection lasers used for fiber-optics is usually rectangular with a maximum dimension less than 10 micrometers permitting efficient coupling into 50 micrometer (micron) core fibers that are becoming the standard for most applications. The emitting area of an LED is usually significantly larger than that of laser with typical diameters ranging from 20 to 50 microns. The larger source area combined with a more divergent emission beamwidth results in relatively poor coupling efficiency with a 50 micron core fiber having an NA in the range of 0.20 to 0.23. The coupling efficiency to a graded index (GI) fiber is generally poorer than to a step index fiber of the same size because the radial variation of the refractive index of the graded fiber causes the NA to decrease as the radial distance from the axis increases.

Most LEDs will not couple more than about 50 microwatts into a 50 micron core GI fiber at 50 to 75% of maximum bias current; however an etched well emitter recently developed by Plessey (HR810F) will couple 150 microwatts into 50 micron core, 0.2NA GI fiber at 150 mA (75% maximum drive). With a 100 micron core, 0.3 NA step index fiber, 750 microwatts can be coupled into the waveguide. Consequently, with this source as well as most other LED sources, it is desirable to use large core fiber to increase the launched power and the analog SNR (recall from equation (3) that the detected signal power is proportional to $(kP_o)^2$).

Increasing the core size of an optical fiber to achieve greater coupling efficiency to an LED results in an increase in the modal dispersion of the fiber and a corresponding decrease in frequency bandwidth. A compromise must be made between optical power and frequency bandwidth. The proper balance is dictated by the specific application, but in many cases it is desirable to choose a fiber diameter and index grading profile that results in a fiber bandwidth comparable to that of the LED.

Bandwidth Considerations

The bandwidth of an optical fiber can be easily related to its dispersion characteristic provided some assumption is made regarding the nature of pulse spreading. For example, it is often assumed that a zero width optical pulse launched into a fiber will spread into a Gaussian shaped pulse as it propagates. In this case the spreading Gaussian optical pulse is described as

$$f(t) = (2\pi\delta^2)^{-\frac{1}{2}} e^{-t^2/2\delta^2} \tag{6}$$

and the full pulse width at the 1/e power points is given by τ_e where

$$\tau_e = 2\sqrt{2}\,\delta \tag{7}$$

A variety of methods are used to describe pulse spreading. These include a specification of (a) full width, half maximum dispersion τ_{FWHM} which is related to τ_e as

$$\tau_e = 1.20\,\tau_{FWHM} \tag{8}$$

(b) full width dispersion at 10% intensity τ_{10} which is related to τ_e as

$$\tau_e = .659\,\tau_{10} \tag{9}$$

and (c) the rise or fall time between the 10% and 90% intensity level $\tau_{r,f}$ which is related to τ_e as

$$\tau_e = 1.68\,\tau_{r,f}. \tag{10}$$

The relationship of these time domain specifications to frequency response is determined by taking the Fourier transform of (6) from which we find the frequency representation of the optical pulse to be

$$F(\omega) = e^{-\omega^2\delta^2/2} \tag{11}$$

The electrical response is proportional to the square of the optical response so that the 3 dB cutoff is given by

$$(\omega\delta)^2 = -\ln 0.5 \tag{12}$$

or $$f_{3dB} = .8326/2\pi\delta \tag{13}$$

or $$f_{3dB} = .375/\tau_e \tag{14}$$

or $$f_{3dB} = .312/\tau_{FWHM} \tag{15}$$

or $$f_{3dB} = .569/\tau_{10} \tag{16}$$

or $$f_{3dB} = .223/\tau_{r,f} \tag{17}$$

To our knowledge these relationships are rarely seen in the published literature except for (14) which is reported in reference [10]. The reader is reminded that $\tau_{r,f}$ is equal to the rise or fall time, not the sum of both.

Since the optical fiber, optical source, and optical detector will have characteristic pulse widths, the 3 dB electrical response for the combined system will be calculated from (13-17) with $\tau = \tau_{eq}$ where

$$\tau_{eq} = [\ \tau^2 \text{ fiber} + \tau^2 \text{ source} + \tau^2 \text{ detector}] \tag{18}$$

and all τ's are expressed in the same form.

A word of caution is necessary when using the full-width, half-maximum dispersion characteristic for an optical fiber that is provided by the manufacturer. Sometimes the pulse dispersion in the fiber is not symmetrical, much less Gaussian. The pulse spreading may be symmetric and well-behaved to the half maximum, but somewhere below this point spreading increases rapidly and irregularly. In this situation the fiber bandwidth calculated from the FWHM data provided will be larger than will be actually achieved. Some fiber manufacturers now provide fiber dispersion measurements at half intensity and at 10% intensity in recognition of this problem.

An additional bandlimiting mechanism in optical fibers is material (chromatic) dispersion in which light waves of different optical wavelength travel at slightly different speeds, thereby arriving at different times at the end of the fiber link. The narrower the spectral width of the source, the smaller will be the dispersive delay of the link. In this respect, the laser with its narrower spectral width has a distinct advantage over the LED when a large bandwidth distance product is required using AlGaAs components. In the 800 to 900 nm range of wavelengths, fused silica fiber has a material dispersion of about .1 to .15 ns/(nm-km), leading to a typical dispersion of 5ns/km for LED sources. At longer wavelengths near 1300 nm, where quaternary device technology must be used, fiber material dispersion becomes so small that the bandwidth of LED-sourced links is limited only by the modal dispersion of the link and the risetime of the source.

In the 800 to 900 nm wavelength range, the bandwidth-distance product for 50 to 60 micron core GI fiber ranges from 200 to 1500 MHz-km depending upon the manufacturer and production cost considerations. 100-micron core, quasigraded index fiber is now readily available with a bandwidth-distance product of 200 MHz-km and as a special order with 400 MHz-km product.

Excess Loss in Fibers

The attenuation specified for an optical fiber is accurate only when the fiber is straight or subjected to a very large winding radius of curvature at low tension and when there is no small radius bending from fiber cross-overs. These conditions are rarely met on a shipping reel of plastic-buffered fiber, and the user of fiber in this state (for example to simulate long data links in a laboratory environment) should anticipate the actual attenuation to be several dB/km larger than specified by the manufacturer.

When the fiber is used in a highly stressed tether-cable, additional loss can be expected from a phenomenon known as microbending. This effect occurs at sites where the fiber is pressed, by internal cable forces, against surface irregularities of adjacent cable elements such as conductors, filler rods, or jacket walls. Subjected to small amplitude bends with small radii of curvature, the fiber exhibits additional loss at the microbends because light rays that are usually contained by total internal reflection are now lost by radiation into the cladding where the attenuation is very high. An additional mechanism for increased loss in a fiber with an undulating path is rapid conversion of low-order spatial modes into higher-order modes that experience somewhat larger attenuation. This explanation is somewhat simplistic, but rigorous theoretical descriptions have been given by many authors such as Gloge [11] and Marcuse [12].

When a fiber is placed into a cable structure with a continuous helical lay to provide strain relief under conditions of cable flexure, radiation loss associated with the continuous fiber path curvature must be held to a tolerable level. Wilkins [13] states that for graded index fibers a lower limit for the radius of curvature of the fiber in a helical lay is 50 mm. In terms of the pitch diameter D_p and lay angle α of the helix, this rule can be written mathematically as

$$D_p / (2 \sin^2 \alpha) \geq 50 \text{ mm} \qquad (19)$$

Wave theory considerations of the evanescent field existing in the cladding at microbending sites suggest that losses may be greater (from microbending) for fibers with a small ratio of cladding thickness to overall diameter. Miller [14] observed this effect in attempts to fabricate laminated fiber ribbon cables and concluded that excess cabling losses decrease with increasing NA and increasing ratio of cladding thickness to core diameter. In attempts to hermetically seal fibers with metal coatings, Rourke and Wysocki [15] found that excess microbending loss, produced undesirably as a consequence of initial fabrication technique, followed an equation of the form

$$L = 48 \times 10^{-6} \ (t/d)^{-3/2} \ (\Delta n)^{-3} \qquad (20)$$

for a kilometer length of fiber, where L is the excess loss (expressed as a ratio), Δn is the core-to-cladding difference in refractive index, t is the cladding thickness, and d is the core diameter.

The mathematical description of microbending loss for optical fibers that are packaged in cable structures seems to follow a much stronger dependence on the relationship between cladding thickness and core diameter. Applying the formal results of Olshansky [16], Gardner et. al. [17] show in very simple terms that the microbending loss resulting from fiber packaging is proportional to a^4/d^6, where a is the core diameter and d is the cladding diameter. D. B. Keck of Corning Glass has found (private communication), through a statistical survey of limited available data, that cabling loss is proportional to a^4, d^5, and $(NA)^{-6}$. From the standard relationship between the NA and refractive indices for a step index fiber

$$NA = \left[n^2(\text{core}) - n^2(\text{cladding}) \right]^{1/2} \tag{21}$$

it follows that for $\Delta n = n(\text{core}) - n(\text{cladding})$ Δn is proportional to $(NA)^2$ to first order approximation in the ratio of $\Delta n/n(\text{core})$. It is therefore apparent that the $(NA)^{-6}$ dependence found by Keck is consistent with the $(\Delta n)^{-3}$ dependence found by Rourke and Wysocki; however, the dependence on cladding diameter found by Keck differs by one unit in the exponent from that predicted by Gardner et. al.

When comparing fibers of different core, cladding, and NA parameters, the comparative performance is given by the ratio R where

$$R = \left(\frac{a_2}{a_1}\right)^4 \left(\frac{d_1}{d_2}\right)^M \left(\frac{NA_1}{NA_2}\right)^6 \tag{22}$$

where M=5 according to Keck and M=6 according to Gardner et.al. If we let fiber 2 be described by 100 micron core diameter, 140 micron cladding diameter, and NA = 0.3 and fiber 1 by 50 micron core diameter, 125 micron cladding diameter, and NA = 0.23 we find that the large-core fiber will exhibit 1.65 times more cable-induced microbending loss than the small core fiber using the a^6 dependence and 1.84 times more loss using the a^5 dependence. Consequently, if a large-core fiber is used in a tether cable optical link because of its superior coupling efficiency with an LED, the advantage may be diminished because of larger microbending loss unless the cladding diameter is increased beyond present standards.

In a poorly constructed fiber-optic cable the path of the fiber may develop periodic waviness because of the presence of discrete pressure points from adjacent cable elements such as armor or conductor wires or because of waviness in the jacket walls of elements against which the fibers lie.

If the fiber path undulates with a spatial periodicity that is nearly equal to that of the mode propagation within the fiber, a resonance may be achieved in which the radiative loss becomes enormous. This condition is realized when the wavelength of the fiber positional undulation is equal to

$$R = K\pi rn/NA \qquad (23)$$

where r = core radius
n = core refractive index
$K = \frac{2}{\sqrt{2}}$ (graded index fiber)
(step index fiber)

Noise and Distortion In Fibers

An optical fiber, as a unique entity, provides a relatively noise-free channel for modulated light waves. Indeed, one of the attractive features of optical fibers is the almost complete immunity to external electromagnetic influences. However, the combination of a multimode optical fiber and a coherent light source (laser) will produce a serious form of noise and distortion in an optical link. A relatively simple explanation of this effect is given below.

Every multimode fiber exhibits some degree of modal dispersion; that is, rays of a different spatial mode (different propagation angle) will arrive at the end of the link with a slight phase delay relative to the optical wavelength. If the fiber is illuminated with a nearly monochromatic (highly coherent) source, the rays arriving at the end of the link will be at the same wavelength but shifted in phase, resulting in an interference pattern. Because the refractive index of the fiber is sensitive to temperature and pressure (flexure and vibration) the interference pattern at the end of the link will not be stationary but will fluctuate analogous to the fluctuating speckle pattern of a helium-neon laser. This effect will occur not only at the end of the link but at every section of the fiber link to a distance equal to the coherence length of the source.

At any interface, such as a fiber-to-fiber connector, the illumination flux density will vary (as a result of the speckle pattern) across the area of the interface. In principle, if all the luminous flux were captured by the receiving fiber, no noise would result. Since there is always some loss at a connection (and even within the fiber itself) the power captured by the receiving fiber will be modulated by the fluctuating speckle pattern. To the extent that the fluctuation is random, the effect at the detector will be added noise. If there is a correlation between the fluctuations of the speckle pattern and modulation of the source, then the resultant intensity fluctuations at the detector will be in the form of time-varing distortion of the modulation waveform. Observations of the electrical output of the optical detector with a spectrum analyzer frequently show variations in the magnitude of a second- or third-order distortion product of 20 dB over time intervals of the order of minutes. Additional discussion of modal noise and distortion in optical fibers can be found in references [18-22].

Although we have attempted to explain the modal noise/distortion phenomenon in terms of spatial filtering (i.e. speckle pattern and loss mechanisms) Rawson [28] reports that transmission of an optical signal through a polarization sensitive element will also provide conditions leading to modal noise. The polarization sensitivity is again linked to changing spatial mode distributions in the fiber which affect not only the speckle pattern but also cause power exchange between polarizations.

The modal noise/distortion problem with multimode fibers does not exist with incoherent sources such as an LED. The problem can be reduced with laser sources by choosing a laser device that has a broad multimode emission spectrum that effectively reduces the coherence length.

An additional complication that we have observed in attempts to use a laser with a broad multimode emission spectrum is that the multimode optical fiber acts as a spatial mode filter that eliminates some of the spectral lines emitted by the laser. Moreover, the filter characteristics are extremely sensitive to fiber position. A minute change in position of a small segment of fiber will drastically alter the appearance of the optical spectrum observed at the end of the link. In fact this effect was so severe that it completely frustrated our attempts to characterize the emission spectrum of the lasers investigated in this report by observing the link output with a Fabry-Perot interferometer. Short lengths of optical fiber (a few meters) also exhibited the filtering effect. The filtering effect, which is very unstable because of rapidly changing spatial mode distributions in the fiber, is a potential source of noise and distortion because the portions of the optical spectrum that are passed by the fiber under differing spatial mode distributions may not transmit equal power.

The use of single-mode optical fiber should, in principle, eliminate the modal noise/distortion problem. However, the small core size (4 microns) presents new problems such as less power coupled from the source than for multimode fiber and more expensive connectors because of the smaller alignment tolerances required at junctions.

ATTRIBUTES OF LASERS AND LEDS

Having considered numerous factors that affect signal transmission at the detector and in the fiber link, we now focus attention on the general attributes of a laser and an LED as a choice of optical source. We will consider factors such as power coupling into fibers, modulation bandwidth, modulation sensitivity, distortion, noise, temperature sensitivity, and lifetime.

Power Coupling Into a Fiber

A solid state injection laser can couple much more power into a small core (say 50 micron) fiber than can an LED because the laser has a greater light generating efficiency, less divergence in the emission beamwidth, an emission area smaller than the cross-sectional area of all (except single mode) fibers, and (as a consequence of small source size) the potential to use collimating and beam shaping lenses to further improve coupling efficiency. The use of lenses to improve coupling between source and fiber

is profitable only when the emitting area of the source is less than that of the fiber core; therefore, for LEDs, coupling lenses are more useful for large core fibers than for small core fibers.

The emission area of a laser is usually rectangular with a maximum dimension of about 10 microns or less. The emission area of an LED of the type used in fiber-optic applications ranges from 20 to 50 microns, with the small area device producing less power but having higher bandwidth and better coupling efficiency [24].

Lasers available from many manufacturers will couple 2 to 3 mW average power into 50 micron core, 0.2NA, GI fibers. However, our experience with analog intensity modulation of lasers has shown that the linear dynamic range usually decreases when the devices are biased above 0.5 to 1.0 mW because of increased distortion and noise. Therefore the potential of coupling several mW of laser power into a fiber may not be as valuable for analog modulation as might otherwise have been anticipated.

The majority of LEDs that are available for fiber-optic applications will typically couple power on the order of tens of microwatts of "usable" optical power into 50 micron GI fibers. Some exceptions to this statement are reported in [24]. We invoke the term "usable" optical power because manufacturers often imply that significantly more power is coupled into the pigtail fiber that is attached to the device. Unfortunately, mode stripping is frequently not used in the manufacturer's measurements so that a significant fraction of the power is carried by high-order modes that will be strongly attenuated in a link with 100-meter or greater length.

An excellent LED presently available from Plessey is the HR810F which will couple 150 microwatts into 50 micron core, 0.2NA GI fiber at 75% maximum drive with cladding modes fully stripped. The same device will couple 750 microwatts into 100 micron core, 0.3 NA step index fiber.

Modulation Bandwidth

Most lasers have a modulation bandwidth of 1 GHz or greater; consequently, for most practical applications the system bandwidth is not limited by the laser source. For laser-driven analog systems with link lengths less than 2 km the detector-amplifier is the predominant bandwidth limiting component. As the bandwidth of the system is increased toward 100 MHz or greater, the detector noise per unit bandwidth increases even when receiver designs as proposed by Personick [25, 26] are used which employ a high impedance, band- limiting front end followed by an amplifier that equalizes the frequency response.

The modulation bandwidth of an LED source is considerably less than that of a laser for two reasons. First of all, the optical flux risetime of the semiconductor device itself is much longer than that of the laser. (Laser Diode, Laboratories IRE 160 series, 14 nsec; ITT T7500 series, 5 nsec; Plessey HR810F, 3 ns). Consequently, a 3 dB electrical modulation bandwidth of 75 MHz is about the maximum to be expected even for very short optical links.

Secondly, the 50% spectral width of an LED is 40 to 50 nm; whereas, for a laser it is only about 1 nm. The material or chromatic dispersion of fused silica fibers is about 0.1 to 0.15 ns/km per nanometer of source spectral width. For a 40 nm spectral width, one kilometer of fiber would have only 62 MHz bandwidth from material dispersion alone. Including the effect of a 3 nsec risetime of an LED source, the system bandwidth would be 48 MHz for a one kilometer link assuming the detector to have a negligibly small risetime. Intermodal dispersion, which will be larger for large core fiber than for small core fibers and larger for step index profiles than graded index profiles, will further limit the bandwidth of the link.

Modulation Sensitivity and Its Impact on Driver Requirements

The modulation sensitivity of laser or LED depends upon the slope of the optical transfer characteristic of the device (optical power vs electrical current) near the bias point (generally chosen near half maximum power). Based on the power coupled into a 50 micron core, 0.23 NA, GI fiber, lasers we have used exhibit transfer characteristic slopes ranging from 70 to 400 microwatts/mA. Since better coupling efficiency to an LED can be achieved with large core fiber, we state corresponding LED transfer characteristic slopes for coupling into 100 micron core, 0.3NA, step index fibers. These range from 1 to 4 microwatts/mA at 100 mA bias.

The data given above indicate that to achieve the same level of optical modulation the LED must be driven 70 to 100 times harder than a laser. The lasers we have tested develop a maximum third-order linear dynamic range at a drive level of about -20 dBm using simple 50 ohm RC coupling into the relatively low AC impedance of the laser device. Using similar RC coupling into an LED, a 70 times larger drive current would require a +17 dBm drive level.

If a 70 dB LDR_3 is required and is achieved at the levels given above for the laser and LED, then the driver amplifier for the laser would require a third-order intercept point IP_3 of +15 dBm or better and the drive amplifier for the LED would require an IP_3 of at least +52 dBm. These IP_3 requirements are easily met for the laser but cannot be met for the LED with commercially available devices. A mitigating factor for the LED is that the system noise level may be up to 20 dB lower than that for the laser-driven system so that comparable performance may be achieved with the LED at a drive of -3 dBm and a driver IP_3 of + 32 dBm, which is achievable with present technology. It is evident, however, that the requirements for the driver of an LED are more stringent than for a laser. The most significant considerations for most applications will be (a) achievement of the required IP_3 and (b) the increased electrical power consumption associated with a large-IP_3 amplifier. The additional cost of the driver for the LED is insignificant in terms of the cost differential between a laser and an LED.

Some relief from the high power requirements for the LED driver can be achieved by transforming impedance from the usual 50 ohm standard to a lower value, thereby achieving better power transfer to the low (AC) impedance of the LED. However, two problems associated with this approach are (a) AC coupling to the LED requires larger capacitors and, more importantly, (b) nonlinearities in the AC impedance of the LED will distort the driving current more as the driver impedance decreases.

Distortion

For all analog systems with LED drivers, the major source of distortion is the nonlinearity of the optical transfer characteristic. This nonlinearity is easily recognizable as a gradual decrease in slope as the electrical current increases. LEDs with LDR_3s as large as 75 dB in 3 kHz bandwidth are reported in the MEASUREMENTS section; corresponding LDR_2s range from 54 to 59 dB. The varying slope of the transfer characteristic causes the detected SNR to decrease as the bias current increases.

For analog systems with conventional multilongitudinal-mode laser drivers, modal distortion (as defined and explained previously under Noise and Distortion in Fibers) is probably the primary source of nonlinearity with slope variations of the transfer characteristic assuming a secondary role. Modal distortion can be reduced by using a laser with a shorter coherence length (laser with a broad multilongitudinal mode structure). This statement is supported by our measurements with a broad spectral width (10 to 20 nm) super-radiant laser diode (General Optronics model GOLS 3000) that has 50 to 70 lines in its emission spectrum. Observations of distortion spectral lines for this device showed no evidence of temporal variations which routinely accompany modal distortion observed on narrower spectral width lasers.

Sladen and Look [27] report that an additional distortion mechanism for the laser-fiber combination is that the far-field emission pattern parallel to the heterostructure junction may change with power level, causing a variation in power coupled into the fiber as a function of optical power or modulation level.

We have observed lasers with LDR_3s up to 63 dB in 3 kHz BW for a link length of 500 meters; corresponding LDR_2s are typically on the order of 50 to 55 dB. For the broad spectral width super-radiant laser, LDR_3s up to 69 dB have been measured.

A point that we cannot overemphasize is that the performance (distortion, noise, modulation sensitivity) of a given type of laser will vary strongly from device to device. A good device cannot be specified by type but must be hand-selected by laboratory testing.

Noise

The LED is a relatively noise free source; the square of the rms noise current at the output of the detector can be made to approach the quantum limit of $2qRP_o$ as defined in equation (3) provided sufficient average optical power reaches the photodetector to swamp its thermal noise.

The laser is a very noisy source for a number of reasons. We have previously discussed (under Noise and Distortion in Fibers) the origin of modal noise when lasers are used with multimode fibers. Hirota and Suematsu [28] report that noise can also be generated by reflections of light from the link back into the laser cavity. Reflections from regions close to the laser cavity produce noise because of phase variations of the reflected light caused by mechanically and thermally induced variations of fiber

refractive index. A different form of noise is generated from reflections from more distant points which randomly create conditions of locking and unlocking in the laser cavity.

Kanada and Nawata [29] also show that noise is created by reflections from the link back into the laser cavity. They point out that periodic fluctuations in the frequency response in integer multiples of $c/2nl$ (c = velocity of light, n = refractive index, l = length of link) can be produced from reflections from the end of the fiber link. In Figure 9 we show the oscillatory noise floor/frequency response resulting from an end reflection from a 500 meter link using a Laser Diodes, Inc. SCW-20 laser. The power spectrum of Figure 9 shows an oscillation approximately every 192 kHz; calculation based on a 500 meter link predicts periodic fluctuations every 200 kHz. The two large, narrow spectral lines are test tones that have no significance for this observation; the periodic fluctuations of the noise floor remain when the test tones are removed. We found that there was a particular bias current for which the fluctuations were a maximum. The oscillatory phenomenon can be eliminated by polishing the end of the fiber at an angle that will prevent capture of the reflected wave.

Finally Kanada and Nawata show that the emission spectrum of a single mode laser can be changed to a multimode structure from light reflected back into the lasing cavity. Mode partition/competition noise is discussed by Ito and Kimura [30], Ito et. al. [31], and Okano et. al. [32].

Our measurements of the ratio of illuminated to dark receiver noise are shown in Figure 10 as a function of frequency for LED (Plessey HR810F, #039) and laser (General Optronics model GOLT) illumination of a MERET R1900 hybrid optical receiver that was biased at 40 volts. The link length was 500 meters for the laser and 620 meters for the LED, and nearly equal power was incident on the photodetector for each link. The data indicate that, relative to the zero illumination noise floor, the laser is about 20 dB more noisy than the LED. From our experience, biasing the laser at higher power does not reduce the noise. The downward slope of the noise data in Figure 10 is caused by a rising noise floor of the detector as the frequency increases.

As previously implied, modal noise and modal distortion can be reduced by decreasing the coherency of the laser which is accomplished by broadening the emission spectrum. In Figure 11 we compare the optical system noise resulting from a conventional multilongitudinal mode laser (ITT type T7591, #151) with that from a GOLS-3000 super-radiant laser diode. The noise is plotted as decibels above receiver dark (thermal) noise as a function of average optical power from the device pigtail (50 micron core fiber) in decibels relative to a milliwatt. In addition to the significantly lower noise of the GOLS-3000 below 0 dBm average power, the most striking feature of Figure 11 is the high variability (slow temporal fluctuation) of the conventional-laser noise contrasted to the very predictable (low variability) noise for the superradiant laser.

Temperature Sensitivity

There is a large contrast in the comparison of the temperature sensitivity of an LED and a laser. The properties of an LED vary slowly with temperature and the device will operate over a wide temperature range without requiring the use of a thermoelectric cooler. For example, the Plessey HR810F diode is specified to have a temperature coefficient of output equal to 0.5%/C and to operate over a temperature range of -40 to 90C.

More complete temperature sensitivity data for an AlGaAs LED is available from the report of Olsen et. al. [33]. From their data we find that the temperature dependence of the output power and the slope of the transfer characteristic are almost identical.

The sensitivities are determined to be:

.7%/C at 20C
.9%/C at 50C
1.1%/C at 70C

The temperature sensitivity of the peak emission wavelength of an LED is about the same as for a laser and is approximately equal to 0.25nm/C.

For AlGaAs laser sources, the lasing threshold current I_{th} depends on temperature exponentially as

$$I_{th} \propto e^{\Delta T/To} \qquad (23)$$

where T_0 equals 150C. This property, combined with a higher temperature sensitivity relative to the LED, forces the user to achieve stable operation by either controlling the temperature of the laser heatsink (usually by a thermoelectric cooler) or by adaptively adjusting the biasing current with the use of an optical feedback circuit to maintain constant average optical power [34].

The temperature sensitivity of the power output of an AlGaAs laser can also be extracted from reference [33] from which we obtain

1.3%/C at 20C
2.2%/C at 50C
4.4%/C at 70C

These data agree with the temperature sensitivity of other AlGaAs lasers such as the Hitachi HLP1000 as determined from product data brochures.

Unlike the LED, however, the slope of the laser transfer characteristic (and hence its modulation sensitivity) is not strongly temperature dependent. Characteristic curves taken at different temperatures tend to show just a displacement or offset from a similar curve at a different temperature with only a slight tendency to develop a decreased slope at high temperatures. Quantitative description of the temperature dependence of transfer characteristic slopes may be device dependent and is not attempted here. Lasers can

be operated at temperature up to 70C; however, temperatures above 40C may have a significant impact on device lifetime. System designers generally strive to keep the laser heatsink temperature below 40C, using a thermoelectric cooler if necessary.

Lifetime

The lifetime of an LED is usually quoted to be about 10^6 hours (114 years). The nominal lifetime of a laser is estimated to range from 10^4 to 10^5 hours (1.1 to 11.4 years). These lifetime projections assume, particularly for the laser, that the device is used in a relatively benign environment. This assumption may not apply in some practical applications, particularly military ones.

When a laser is used for analog modulation, it is usually biased well above threshold. Because of the large slope of the optical transfer characteristic, only a few additional milliamperes of current are required to drive the laser to maximum permissible output power. Because lasers are so sensitive to overdrive (including short-term transients), power supplies used for biasing must be transient snubbed to prevent device damage or destruction even in the laboratory. Damage caused by a transient may range from slight degradation (usually in the form of an increased threshold current) to total destruction, depending on the magnitude and duration of the transient. The usual failure modes are thermal fusing of the device (or its contact wire) and optical facet erosion.

The very delicate disposition with respect to transients may put the solid state injection laser near the top of the list of devices most susceptible to EMP (electromagnetics pulse interference). The impact of EMP on laser lifetime may be a greater concern for military applications than extension of its nominal 10^4 to 10^5 hour lifetime in non-EMP environments. The LED will be much more immune to EMP because (a) larger current swings can be tolerated, (b) response to transients is slower, and (c) since lower optical power is involved, optical facet destruction is less probable.

MEASUREMENTS

The measurements of optical source characteristics will be presented separately for LEDs and lasers. In each case the presentation will begin with a tabular summary of linear dynamic ranges measured under different conditions. Following the summary, a detailed explanation of the data entries will be made when warranted, and other source properties of interest, such as frequency response, and transfer characteristic will be presented.

LEDs

The LEDs were selected primarily on the basis of their potential for coupling a large amount of optical power into a 100 micron core fiber. Devices tested were the Plessey HR810F2, Laser Diode Laboratories, Inc. IRE160FA, and Motorola MFOE108F. There are certainly many other candidate devices that we have not had an opportunity to evaluate. The characteristics of the selected LEDs are given on the following page.

Plessey HR810F2 LED

- Structure: Etched well
- Source dimensions: Not specified
- Wavelength: Typically 850 nm
- Spectral width (50% power): 40 nm
- Output power (manufacturer's claim): 750 W at 150 mA into 100 micron core step index, 0.3 NA fiber; 150 W at 150 mA into 50 micron core, graded index, 0.2 NA fiber.
- Optical rise time: 3 ns
- Maximum forward current: 200 mA
- Cost: $825 (1982)

Laser Diode Inc. IRE-160FA LED

- Structure: Etched well
- Source dimensions: Not specified
- Wavelength: Typically 820 nm
- Spectral width: (50% power) 40nm
- Output power (manufacturer's claim): 300 to 500 microwatts into 125 micron core, step index, 0.3 NA fiber.
- Optical rise time: 14 ns
- Maximum forward current: 150 mA
- Cost: $225 (1982)

Motorola MFOE108F

- Structure: Not specified
- Source dimensions: Not specified. Output is from a 200 micron 0.5NA light pipe compatible with AMP connector #227240-3 and Amphenol connector #905-135--5000
- Wavelength: Typically 812 nm
- Spectral width (50% power): 35 nm
- Output power (manufacturer's claim): 1.5 mW into light pipe
- Optical rise time: Typically 15 ns
- Maximum forward current: 200 mA
- Cost: $27.50 (1981)

The summary of linear dynamic ranges (as defined in the INTRODUCTION) measured for these devices is presented in Table 1. The column labels are identified as:

- I_B: The bias current for the LED
- P_O: The average optical power measured at the output of a short 100 micron core pigtail fiber with no modestripping.
- P_R: The average optical power measured at the output of the link.
- f_1, f_2: The frequencies of the two tones used for intermodulation tests.
- LDR_2: Measured linear dynamic range based on system noise in 3 kHz bandwidth and second-order intermodulation products of form $f_1 \pm f_2$
- LDR_3: Measured linear dynamic range based on system noise in 3 kHz bandwidth and third-order intermodulation products of form $2f_1 \pm f_2$ and $2f_2 \pm f_1$

Measurements with the Plessey #042 LED indicate an LDR_2 of 58.2 dB and an LDR_3 of 75.2 dB near 6 MHz using a link length of 620 meters of Corning SDF fiber (100 micron core, step index, input NA = 0.3, 25 MHz-km bandwidth-distance product, 4.7 dB/km attenuation at 850 nm). The rather large power

Table 1 — Summary of Linear Dynamic Range Measurements for LEDS

DEVICE ID		I_B (mA)	P_o (W)	P_R (W)	LINK LENGTH (Meters)	f_1 (MHz)	LINEAR DYNAMIC RANGE IN 3 kHz BW f_2 (MHz)	LDR_2 (dB)	LDR_3 (dB)
PLESSEY HR810F2 (#042)	a	100	*553	104	620LC	6.0	6.1	58.2	75.2
	b	"	"	37	500SC	"	"	52.5(1)	69.8(1)
	c	"	"	"	"	"	"	53.7(2)	71.4(2)
	d	"	"	"	"	70.0	70.2	--	65.0(1)
	e	"	"	"	"	"	"	--	68.8(2)
(#039)	f	75.3	*485	127	620LC	20	21	54.2	75.5
	g	100	*600	154	"	"	"	54.2	75.0
	h	150	*760	195	"	"	"	54.0	73.9
	i	100	*600	154	"	10	17	56.0	--
LASER DIODES INC IRE 160 FA (#1)	j	100	*185	62.1	620LC	1	4	58.0	75.2
	k	"	"	"	"	20	25	53.4	71.0
	l	"	"	"	"	69.4	70	--	58.5
(#2)	m	100	--	36.2	620LC	1	4	54.3	71.0
	n			"	"	20	25	54.5	70.0
(#3)	o	100	*154.5	39.7	620LC	1	4	59.2	72.3
	p	"	"	"	"	20	25	59.5	71.2
MOTOROLA MFOE108F	q	100	*104.5	24.5	620LC	1	4	48.6	60.0
	r	"	"	"	"	20	25	46.2	63.7

NOTES:

* NO MODE STRIPPING USED

1. PERFORMANCE LIMITED BY THERMAL NOISE OF RECEIVER
2. POTENTIAL QUANTUM LIMITED PERFORMANCE

LC LARGE CORE FIBER (100 MICRON CORE, STEP INDEX, 0.3NA)

SC SMALL CORE FIBER (50 MICRON CORE, GI, 0.21NA)

loss of 7.3 dB from input to output of the link is caused by (a) an overstatement of P_0 because modestripping was not used in this measurement, (b) microbending loss on the fiber spool, and (c) excess loss in the fusion splices (experienced some trouble with air bubbles when fusing this fiber).

Measurements corresponding to rows (b) and (c) of Table 1 were made near 6 MHz frequency with a 500 meter link of small core fiber (ITT graded index, 50 micron core, 0.21NA, 0.3 ns/km dispersion at 900 nm, 3.5 dB/km attenuation at 820 nm) in order to form a basis of comparison for measurements at 70 MHz with the same fiber. Values of LDR_2 and LDR_3 obtained with the small core, fiber were limited by operation near the thermal noise of the receiver (quantum noise 2.4 dB below thermal noise). Values of LDR reported in row (c) of Table 1 represent the performance that would be achieved at 6 MHz with small core fiber if the receiver were dominated by quantum noise. These values should be comparable to the LDRs reported in row (a) but fall short by 3.8 dB for LDR_3 and 4.5 dB for LDR_2 (causes for this have not been identified). The LDR_3 measured near 70 MHz is 65 dB (quantum noise 5.9 dB below thermal noise) as shown in row (d), with a potential LDR_3 of 68.8 dB (row (e)) for quantum noise-limited operation.

The frequency response of a 500 meter link of small core fiber and a 620 meter link of large core fiber with the Plessey HR810F2 LED is shown in Figure 12. The fall-off of the response with the small core fiber is caused by the risetime of the LED and the material dispersion of the fiber. The 4.5 dB loss in response at 70 MHz accounts for some of the loss in LDR_3 measured at this frequency.

The fall-off of the response for the large core fiber is a result of the risetime of the LED, the material dispersion of the fiber, but, primarily, the modal dispersion of the step index fiber. The slight rise in response after 66 MHz represents the damped oscillatory response characteristic of a delay-line filter where, in this case, the delay is associated with different propagation modes in the fiber. The 17 dB loss of this fiber at 70 MHz explains why we used a small core fiber for the high frequency measurement.

Presently, 100 micron core fibers with a quasi-graded-index profile are available with 200 MHz-km bandwidth-distance product. This type of fiber should permit an LDR_3 of close to 69 dB (as reported in row (e) of Table 1) to be achieved in operational systems at 70 MHz.

The optical transfer characteristic for the Plessey HR810F2 (#042) LED is shown in Figure 13. The nonlinearity is obvious but apparently is of a form that results in low third-order distortion. Ignoring considerations of distortion, the decreasing slope, as the current increases, indicates that there may be a particular bias current for analog modulation that provides a maximum SNR. This point will probably be near the current that results in quantum noise comparable to thermal noise at the receiver. At substantially larger bias current the diminishing slope will reduce the modulation sensitivity, hence SNR.

The linear dynamic range of the Plessey #039 device was determined at three different bias currents and at a frequency near 20 MHz. The values of LDR_3 are very close to that obtained for the first Plessey LED (row (a) of Table 1). The values of LDR_2 are about 4 dB less than observed for the first device. At test frequencies of 10 and 17 MHz the LDR_2 was 2 dB higher than at 20 and 21 MHz. The performance appears to be about 1.6 dB better at 75 mA bias than at 150 mA. The optical transfer characteristic for this device is shown in Figure 14 and is qualitatively similar to that of device #043.

The LDR_2 and LDR_3 measured for the Laser Diodes, Inc. IRE-160FA LED at frequencies of 1 and 4 MHz were almost identical to the values determined for the Plessey device (row (a) of Table 1). At test frequencies of 20 and 25 MHz the LDRs decreased about 4.4 dB, almost in direct proportion to the diminished frequency response at these frequencies (Figure 15). Near 70 MHz the LDR_3 decreases to 58.5 dB because of the reduced reponse of the source-fiber combination. The optical transfer characteristic is shown in Figure 16 and is qualitatively similar to that of the Plessey LEDs except that only about half as much optical power is coupled through the link.

The other IRE-160FA LED's (devices # 2 and 3) coupled slightly less power into the fiber than did #1 device and had LDRs either a few dB better or a few dB worse depending on the particular device, frequency, and order of distortion. Frequency response and optical transfer characteristic were qualitatively similar to the characteristics of the IRE-160FA (#1) LED.

The Motorola LED was examined primarily because of its low cost and advertised high power output (1.5 mW into attached light pipe at 100 mA). Coupling efficiency from the 200 micron diameter, 0.5 NA light pipe into a 100 micron diameter 0.3 NA fiber is poor (10.5 dB loss from equation (4)). The maximum amount of power we could couple into a few meters of our 100 micron, 0.3NA fiber was 104.5 microwatts without any modestripping, indicating a coupling loss of at least 11.6 dB. Measured LDR_3s were 10 to 15 dB less than for the previous devices; LDR_2s were 6 to 10 dB less. The optical transfer characteristic is shown in Figure 17 and the frequency response with our 100 micron core fiber in Figure 18.

Our survey of high-power, fiber-coupled LEDs is certainly far from representing an all-inclusive effort; however, we are not aware of any other devices that might offer better performance. In terms of light coupling ability and linear dynamic range, the Plessey HR810F2 is the best device we have seen.

Laser

The characterization of laser performance is more difficult and less precise than that for LEDs. The reasons for this have been discussed previously under "ATTRIBUTES OF LASERS AND LEDS." Recall that with a laser source, system noise depends upon coherent modal interference in the fiber, spatial filtration by the fiber, reflections from the link back into the lasing cavity, longitudinal mode-partition/competition, and stable biasing.

The noise and distortion characteristics of a laser-driven multimode fiber link are not stationary but meander slowly with time because of minute changes in the link environment such as temperature, fiber position, and vibration spectrum. The use of a laser with a broad optical emission spectrum such as the super-radiant GOLS-3000 will reduce, the magnitude and variability of the noise/distortion problem.

As stated previously, the performance of a particular type of laser varies strongly from device to device. High performance devices cannot be ordered by model number but must be hand-selected by laboratory testing. An exception to this statement may apply to the broad spectrum super-radiant laser which may exhibit more predictable performance from device to device; however, we have had experience with only one super-radiant device and thus lack the basis for such a generalization.

All our procurements of lasers for linear dynamic range testing specified that the devices be hand-picked by the manufacturer to have a broad multilongitudinal mode emission spectrum with 4 to 5 modes having comparable output power at a level of 1 to 2 mW coupled into the fiber. Attempts to confirm the multimode structure at NRL by coupling the output of the fiber into a scanning Fabry-Perot interferometer were a frustrating failure because the spatial mode filtration of the fiber prevented the attainment of stable and reproducible spectra. Interestingly, but inexplicably, the spectra from the ITT lasers were considerably more stable and reproducible than those from lasers obtained from Laser Diodes, Inc.

In the investigation of the lasers, the measurement of LDR_3 was considered to be of prime importance. If a device with large LDR_3 could be found, then measurement of the LDR_2 would also be conducted. Prior to embarking on this measurement program our experience with lasers was that an LDR_3 of about 62 dB in 3 kHz bandwidth could be achieved; therefore, the purpose of the measurement program was to identify sources with larger LDR_3. For all except the GOLS-3000 laser, the LDR_3 performance was disappointing; consequently, few measurements of LDR_2 were made.

Communication with Laser Diodes, Inc. revealed that the SCW-20F (#33) device was actually a single-mode device rather than multimode; however, the (unstable) spectra observed with the Fabry-Perot interferometer at the output of a 500 meter link indicated a multimode emission structure. In this case the multimode structure probably originates from reflected light from the link back into the laser cavity (an effect reported by Kanada and Nawata [29]).

The summary of linear dynamic ranges measured for a variety of laser devices under various bias conditions is shown in Table 2. Since the performance of a laser should not be a strong function of frequency, all but a few measurement were conducted near the standard intermediate frequency of 70 MHz which was a region of particular interest to the authors. Performance at lower frequencies should be comparable or slightly better. At higher frequencies performance will degrade slowly because of increased detector noise. Measurement of LDR_3 at 400 MHz with the General Optronics laser, extracted from reference [35], shows a 4.5 dB decrease from the value measured at 70 MHz.

Table 2 — Summary of Linear Dynamic Range Measurements for Lasers

LASER ID	I_B (mA)	I_B/ Ith	P_{out} (W)	LINK LENGTH (Meters)	LINEAR DYNAMIC RANGE RANGE IN 3 kHz BW f_1 (MHz)	f_2 (MHz)	LDR_2 (dB)	LDR_3 (dB)
GENERAL	92*	--	500	113	68.7	70.0	49.5	63.6
OPTRONICS	--	--	--	550	399.7	400.0	--	59
GOLT (7033-174)								
GENERAL	90.0	***	460	520	10.0	10.1	50.6	69.3
OPTRONICS	110.0	***	1000	"	"	"	50.0	68.2
GOLS-3000	90.0	***	460	"	70.0	70.1	--	68.2
	110.0	***	1000	"	"	"	--	66.2
LASER DIODES INC SCW-20F (#225)	101.7	1.03	450	550	69.7	70.0	--	57.3
LASER	125.0	1.040	760	500	69.6	69.8	--	52.0
DIODES	130.0	1.088	1450	"	"	"	--	55.0
INC	134.0	1.121	2000	"	"	"	--	55.00
SCW-20F (#131)								
LASER	28.1	1.014	154	500	69.6	69.8	--	57.5
DIODES	28.5	1.029	308	"	"	"	--	59.5
INC	28.8	1.040	423	"	"	"	--	54
SCW-20F	30.0	1.083	885	"	"	"	--	50
(#33)	31.0	1.119	1270	"	"	"	--	40
ITT, EOPD	69.4	1.036	290	2	69.5	69.8	--	63.7
T7591	70.0	1.045	317	"	"	"	--	68.2
(#151)	72.9	1.088	579	"	"	"	--	69.5
	73.9	1.103	669	"	"	"	--	69.5
	75.5	1.127	814	"	"	"	--	66.0
	76.6	1.143	904	"	"	"	--	61.3
	70.3	1.049	344	500	"	"	--	63.2
	70.5	1.052	362	"	"	"	--	58.8
	83.5	1.246	1540	"	"	"	--	53.3
	69.5	1.037	272	500**	"	"	--	63.0
	70.5	1.052	362	"	"	"	--	62.0
	71.5	1.067	452	"	"	"	--	60.5
	73.5	1.097	633	"	"	"	--	58.5
	76.0	1.134	859	"	"	"	--	56.0
ITT-EOPD	88.0	1.173	890	500	69.6	69.8	--	65
T7591	89.0	1.187	967	"	"	"	--	"
(#153)	92.4	1.232	1180	"	"	"	--	61
	95.0	1.267	1330	"	"	"	--	60

*Current into electronics module. Actual bias current will be less.
**End of fiber polished with 10% angle to reduce end reflections.
***Lasing threshold not well defined.

The largest LDR_3 with a 500-meter link length was obtained with the GOLS-3000 laser. As will be seen later under device characteristics, the optical transfer characteristic for the GOLS-3000 is considerably less linear than that for the other lasers evaluated. The larger LDR_3 for the GOLS-3000 is attributed to the absence of observable modal effects, specifically noise and distortion. A comparison of noise between the GOLS-3000 and the ITT T7519 (#151) lasers has been shown previously in Figure 11.

The effect of link length on LDR_3 is dramatized by the measurements taken with a 2-meter link length as apposed to 500-meter link length for the ITT T7591 (#151) laser. An LDR_3 of 69.5 dB was obtained for the short link length, but the maximum that could be achieved with a 500-meter link was about 63 dB. The reduction in performance was caused primarily by noise added to the system from the interaction of the laser and the longer link. Noise data are presented in Figure 19 for both links as a function of the ratio of bias current to lasing threshold current I_B/I_{th}. Not only is the noise larger for the longer link, but the variability in noise (probably a very slow temporal variation) is also larger.

All of the data presented in Table 2 indicate a trend toward lower LDR_3 for increasing I/I_{th} following attainment of a maximum value at low I/I_{th} (usually less than 1.1). This behavior might be anticipated on the basis of the tendency of the noise to increase with I/I_{th} and the realization that the device must be biased somewhat above threshold to achieve linearity with analog modulation.

All lasers evaluated in this study were operated at ambient temperature and heat generated by the device was removed by mounting to a massive heat sink. The General Optronics laser was purchased with an optical feedback stabilization circuit that maintained a constant (but adjustable) average power output and was insensitive to temperature or power supply variations. All other laser devices were held at a constant optical bias by stabilizing the temperature with the thermal mass and dissipative properties of a massive finned heatsink and by close monitoring of the biasing current.

Frequency responses are not presented for the laser-driven links because the bandwidths of the laser and the fiber (for moderate distance links, say 2 km or less) generally exceed the bandwidth of the detector-amplifier combination if high sensitivity is required. Laser-driven fiber-optic systems with bandwidths of several hundred megahertz can be constructed, but a larger thermal noise spectral density will exist in the detector-amplifier than would occur at smaller bandwidths. For a given link configuration, the optical power budget and noise properties of the source or source-fiber combination will determine the maximum practical bandwidth for a well-designed detector-amplifier system. If the detector-amplifier is allowed to have larger bandwidth, the system noise will be dominated by the thermal noise of the detector rather than by the noise associated with the optical flux (the ideal condition).

Characteristics of the individual laser sources are presented below to the extent revealed by the manufacturer. All lasers are AlGaAs heterostructure devices.

General Optronics Model GOLT

- o Waveguide dimensions: 380 microns long X 8 microns wide X 0.2 microns high
- o Wavelength: 830 nm
- o Threshold current; 90-100 mA at 25 C
- o Mode pattern: Single transverse mode, multiple longitudinal modes
- o Spectral width (50% power): Less than 1 nm.
- o Beam divergence: 45^{o} vertical, 10^{o} horizontal
- o Optical risetime: Less than 0.7 ns
- o Mirror Coating: Dielectric layer passivation.
- o Cost: $3,230 (1981) with fiber pigtail and optical feedback

This particular laser was the best performer from a total of five devices purchased from the General Optronics GOLT and GO ANA series. Some of these devices produced only a 55 dB LDR_3//3 kHz. The optical transfer characteristic was not determined for this laser because the measurement would have required modifying the package electronics to defeat the optical feedback circuitry.

GENERAL OPTRONICS MODEL GOLS-3000
(limited data available)

- o Threshold current: Threshold is very rounded and imprecise (see Figure 20).
- o Mode pattern: 50 to 70 longitudinal modes

  Spectral width: 10 to 20 nanometers
- o Cost: $1,350 (1982) with fiber pigtail and internal optical detector monitor.

The optical transfer characteristic for this device is shown in Figure 20.

Laser Diodes Laboratories, Inc. Type SCW-20F

- o Source size: 0.2 x 7.0 microns
- o Wavelength: Device # 225: 811 nm
  Device # 131: 814 nm
  Device # 33: 862 nm

- Threshold current. Device # 225: 98.7 mA at 25 C
  Device # 131: 119.5 mA at 26.5 C
  Device # 33: 27.7 mA at 30 C

- Mode pattern: Single transverse mode.
  Device #33 had single longitudinal mode; others had multiple longitudinal modes with 0.4 nm spacings.

- Spectal width: Less than 1 nm

- Beam divergence: 10 x 35 degrees

- Optical risetime: 100 to 800 ps

- Mirror coating: Passivated

- Cost: $1000 (1981) with fiber pigtail

Optical transfer characteristics for these lasers are shown in Figures 21-23.

ITT, EOPD Type T 7591

- Structure: Channel Substrate Planar

- Source size: Not specified

- Wavelength: Device # 151: 850 nm (measured)
  Device # 153: 840 nm nominal

- Threshold current: Device # 151: 67 mA at 27 C
  Device # 153: 75 mA at 31.5 C

- Mode pattern: Single transverse mode; multiple longitudinal modes; 0.4 nm spacing between longitudinal modes

- Spectral width (50% power): 2 nm

- Beam divergence 20 x 40 degrees

- Optical risetime: Less than 1 ns

- Mirror coating: Passivated

- Cost: $600 (1982) with pigtail fiber

The optical transfer characteristics for these devices are shown in Figures 24 and 25.

SUMMARY AND CONCLUSIONS

We have defined the linear dynamic range (LDR) of an analog system as the range in decibels between the drive level required for a unity SNR in a stated bandwidth and the level required for a unity distortion-to-noise ratio for a specified order of distortion. For an LED source, the LDR in an analog fiber-optic system is limited by the amount of optical power coupled into the fiber and the linearity of the optical transfer characteristic. For all lasers studied (except the GOLS-3000 super-radiant device) LDR is limited primarily by interaction between the laser and multimode fiber link which causes excessive noise and distortion. For the less coherent GOLS-3000 super-radiant device, modal effects were not observed and LDR is probably limited by the nonlinearity of the optical transfer characteristic.

For an LED source, LDR_3s up to 75 dB in 3 kHz bandwidth and LDR_2s up to 59 dB in 3 kHz bandwidth have been measured at frequencies up to 20 MHz with a link length of 500 to 600 meters. A single measurement of LDR_3 at 70 MHz with a 500 meter link length indicated that the LDR_3 dropped from 75 dB to near 69 dB; reduced performance is anticipated above 70 MHz because of the optical risetime characteristic of the LED source.

For lasers (other than the low coherency super-radiant device), LDR_3s up to 65 dB in 3 kHz bandwidth have been measured at 70 MHz with a link length of 500 meters; however, many devices exhibit poorer performance. The GOLS-3000 super-radiant device produced an LDR_3 up to 68.2 dB at 70 MHz and up to 69.3 dB at 10 MHz with a 500-meter link length. Measurements at 400 MHz with the General Optronics model GOLT laser indicated an LDR_3 of 59 dB. Although only a few measurements of LDR_2 were presented for the lasers, our experience is that values ranging from 50 to 55 dB can be anticipated. Because of the wide frequency response of the laser we expect little change of the LDRs with frequency, except that the detector-amplifier performance will degrade as the frequency increases (particularly noticeable above 100 MHz for our links). The large spectral width of the GOLS-3000 laser (assume 15 nm) limits its potential bandwidth-distance product to about 166 MHz-km from fiber material (chromatic) dispersion.

When an LED is considered for use as a source for an analog link, factors other than linearity must be considered. Large core fiber may be required in many applications to get sufficient optical power to the detector. This fiber may be significantly more susceptible to microbending loss when packaged in a cable structure than will be the standard 50 micron core, 125 micron cladded diameter fiber. Microbending loss is believed to be proportional to $a^4/(d^M\ NA^6)$ where "a" is the core diameter, "d" is the cladded diameter, M is in the range of 5 to 6, and NA is the numerical aperture. The larger microbending loss may negate the initial advantage of greater source coupling efficiency with large core fibers.

A second important factor is the third-order intercept requirement for the amplifier used to drive the LED. For 50 ohm RC coupling to the LED, a drive level of about 0 dBm is required to achieve an LDR_3 of 75 dB. This requires the third-order intercept for the amplifier to be 37.5 dBm relative to the output and necessitates the use of a medium power, high performance amplifier. Impedance transformation can be used to decrease the power demand

on the driver; however, variations of LED impedance with modulation current will make a larger contribution to distortion when low impedance drivers are used.

Finally, the frequency bandwidth must be considered. The maximum bandwidth will be determined by the risetime of the LED and will generally not be more than about 75 MHz. Material and modal dispersion of the link will further limit the bandwidth. Material dispersion for fused silica is about .1 to .15 ns/(nm-km) which, for a typical 40 nm LED spectral width, results in a dispersion of about 5 ns/km. Modal dispersion for 100 micron core fibers is less than 1.6 ns/km (FWHM) (200 MHz-km bandwidth) for quasi-graded index cores.

In some cases a laser may be chosen as the optical source because of (a) the ability to couple more power into a small core fiber, (b) larger modulation bandwidth, (c) narrower spectral width, and (d) less stringent requirements on the driving amplifier. Stacked against these desirable attributes are the disadvantages (a) the lifetime of the laser may be severely jeopardized in an EMP environment, (b) good devices cannot be ordered by model number but must be selected by LDR testing with the actual fiber link of interest, (c) interaction between the laser cavity and the multimode optical link causes increased noise and distortion by several mechanisms and defeats the otherwise high potential for the laser source, and (d) temperature sensitivity will in many applications require thermo-electric cooling to prevent disminished lifetime, provide stable operational conditions, and limit drift in the emission wavelength (particularily if optical wavelength division multiplexing is used).

In general it is not possible to state that one type of source is better than the other unless the specific application is known. The information needed to make the decision for a given application is given in this report and supporting references.

We recommend that analog modulation of fiber-optic links be avoided where possible. An exception to this statement can be made for relatively simple links where a single carrier is used and a large linear dynamic range and/or high fidelity is not required. If multiple, analog modulated, FDM carriers are to be superimposed on a single fiber-optic link, then a significant improvement to the link performance can be achieved by adding an intermediate process of converting all analog carriers to frequency modulated carriers.

If the modulating source for an analog link is a signal from a radio antenna, then very large LDRs are necessary to allow recovery of a weak desired signal in the presence of a strong interfering signal that falls within the IF passband that drives the optical source. Particularly sensitive to this problem are military communication systems that face the prospect of intentional jamming. When faced with the relatively limited LDRs characteristic of LEDs and lasers and when forced to use analog modulation, the system designer must resort to every trick in the bag to preserve LDR headroom. Available techniques include conversion to an FM carrier, hard-limiting (followed by bandpass filtering) of angle modulated carriers prior to introduction to the fiber-optic link, and optical summing of multiple FDM carriers. Obviously, well designed automatic gain control (AGC) circuits are needed to assure optimum system performance; however, AGC cannot improve the instantaneous LDR limit imposed by the LED or laser.

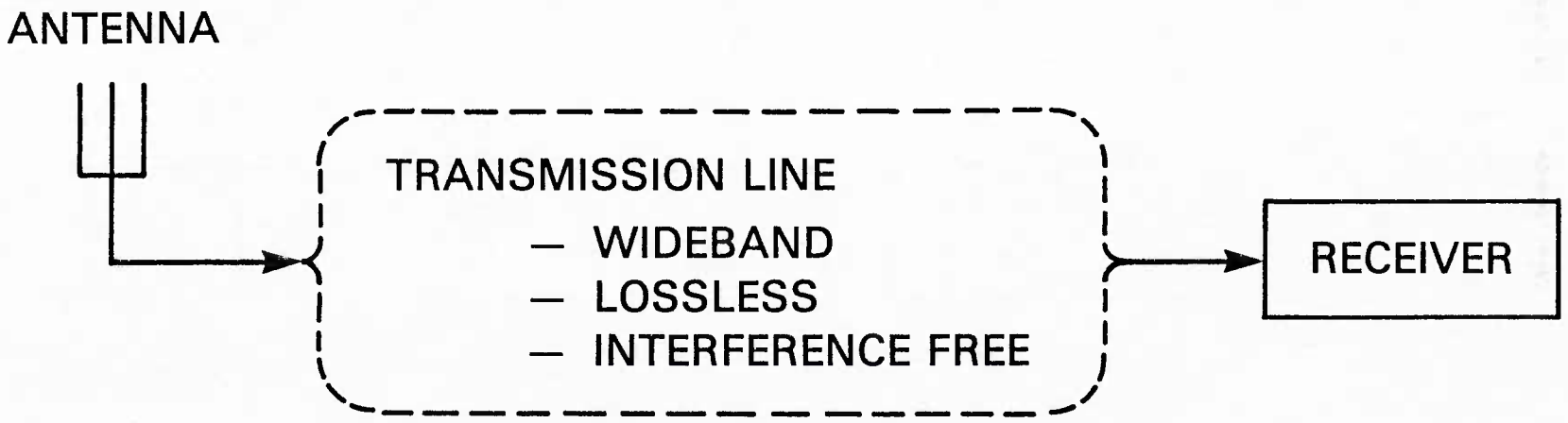

Fig. 1 — The ideal link between an antenna and a distant signal processor.

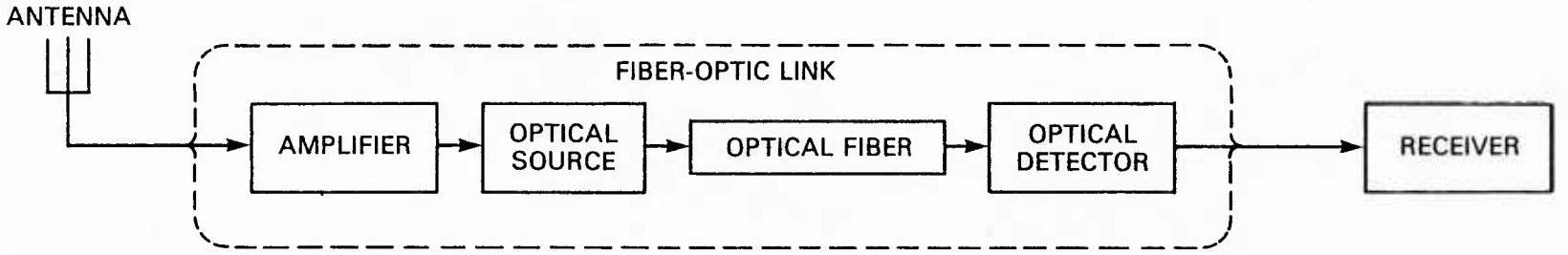

Fig. 2 — Fiber-optic link between an antenna and a signal processor: the novice's folly.

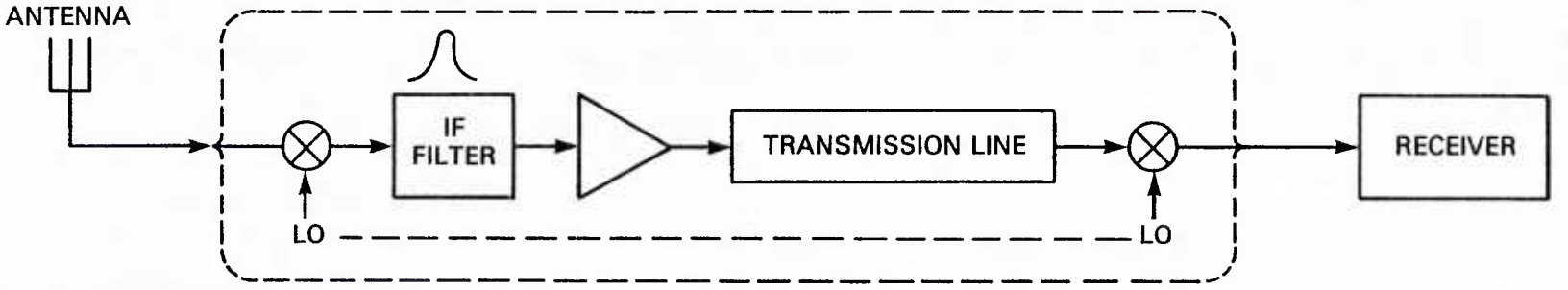

Fig. 3 — A practical compromise to the ideal link between an antenna and a distant signal processor.

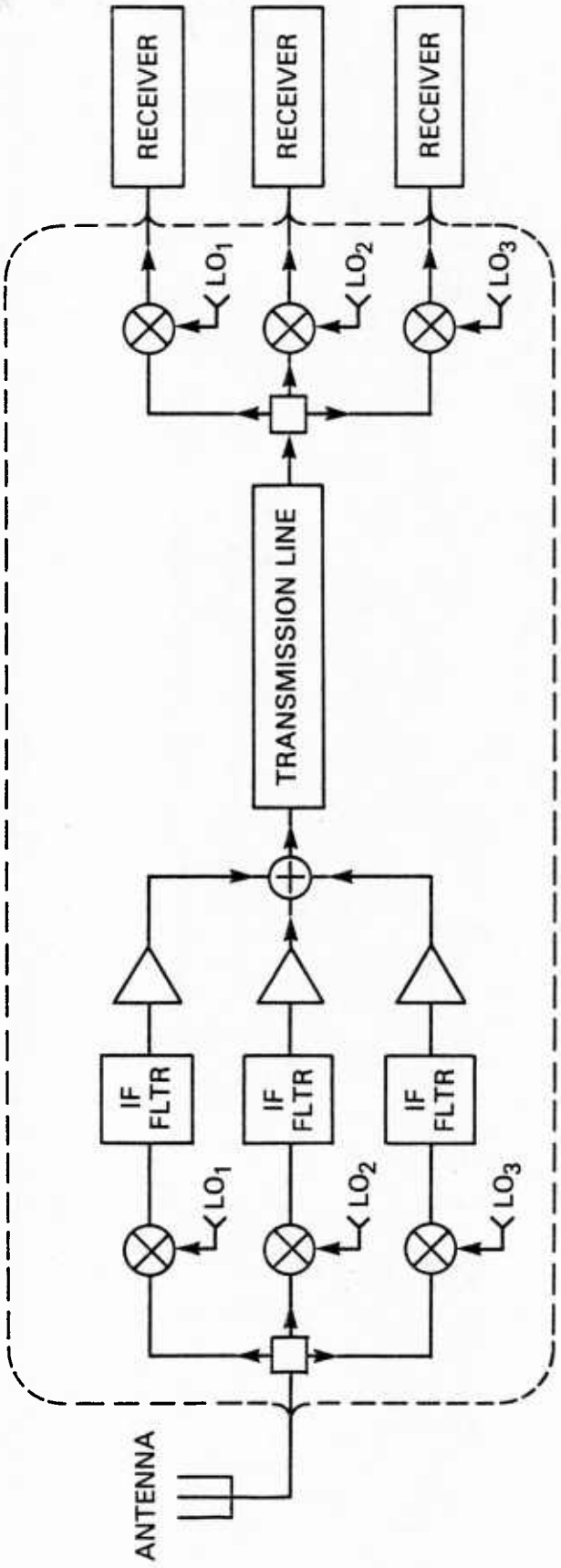

Fig. 4 — The practical link with frequency-division multiplexing (FDM).

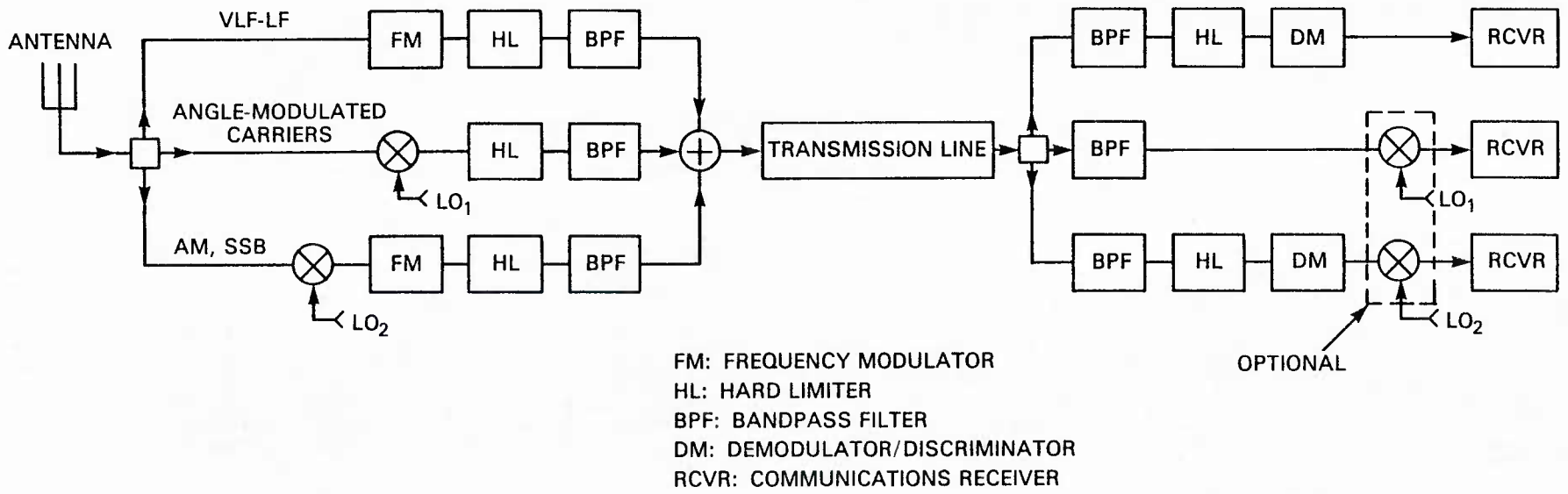

Fig. 5 — The practical FDM link with carrier amplitudes minimized.

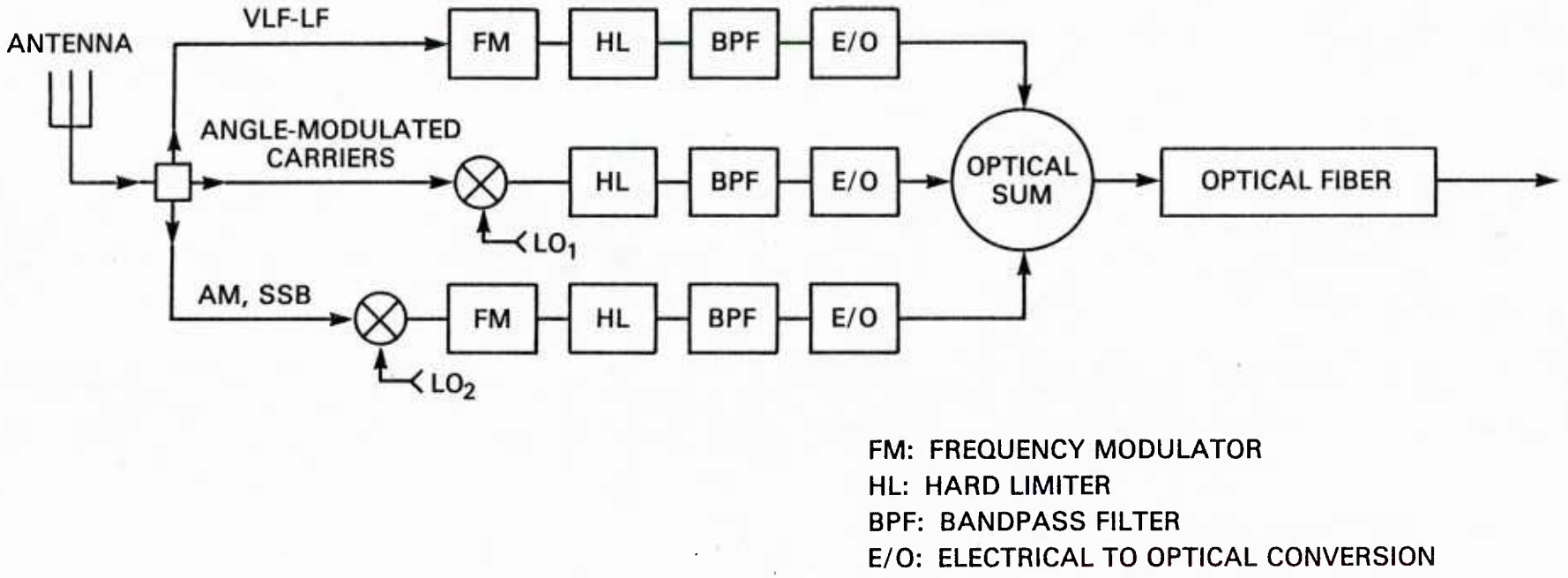

Fig. 6 — A fiber-optic FDM link that reduces intermodulation products between carriers by optical summation.

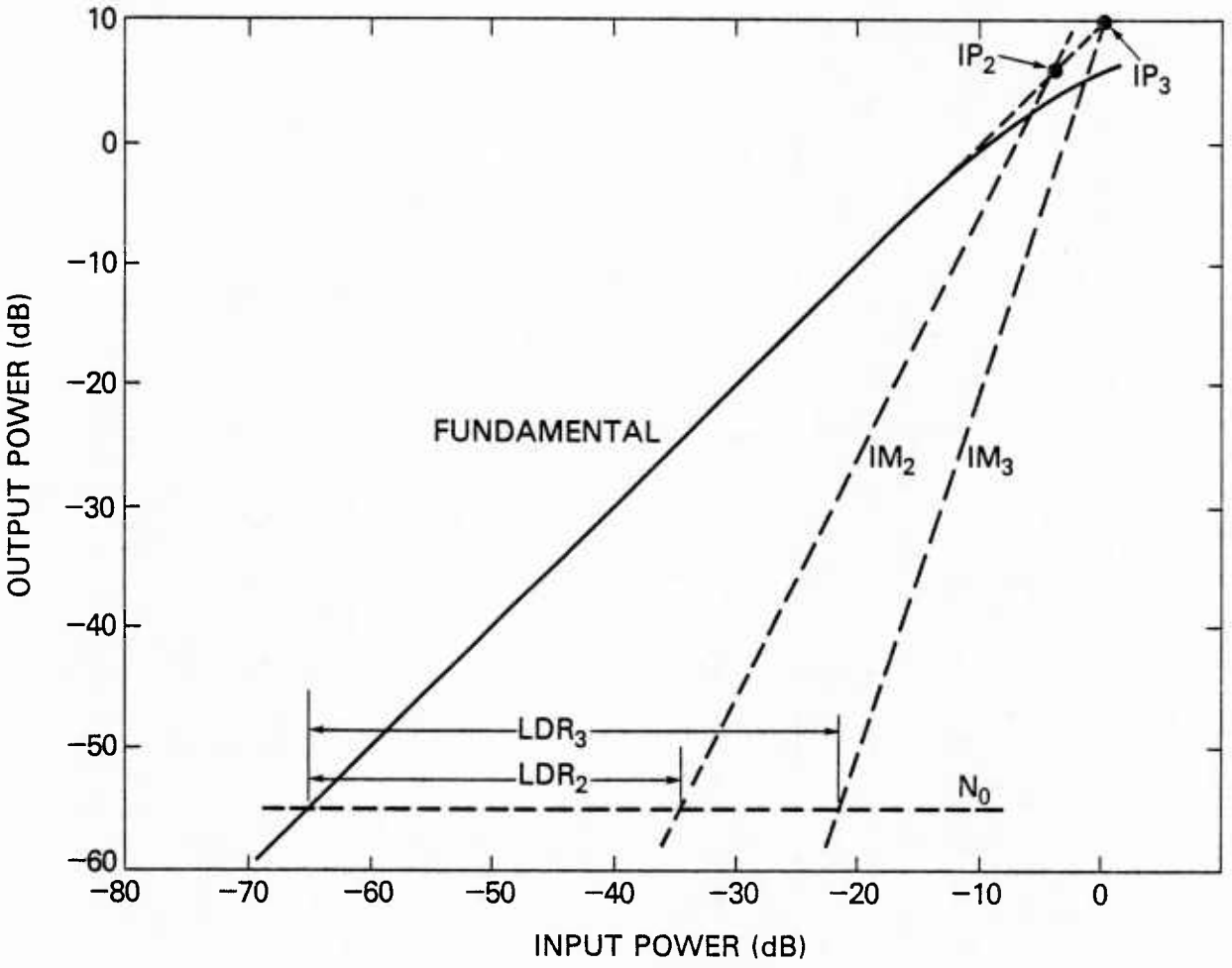

Fig. 7 — Graphical relationship between the intercept points, the input/output transfer characteristic, the intermodulation characteristics, the noise floor, and the linear dynamic range for an electronic or electro-optical component.

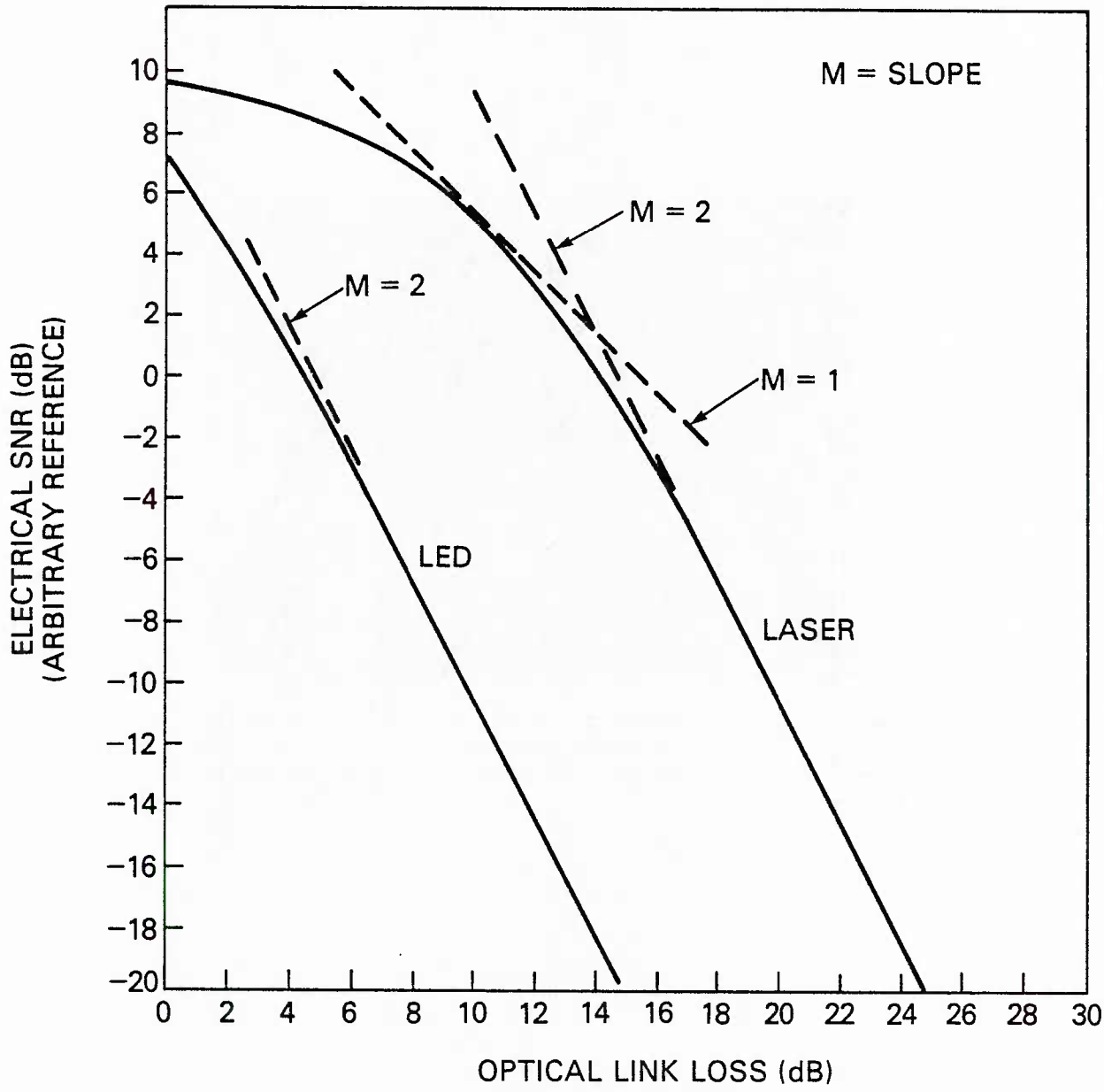

Fig. 8 — Comparative performance between a laser and an LED based on a simple model of signal-to-noise ratio and three reasonable assumptions (see text).

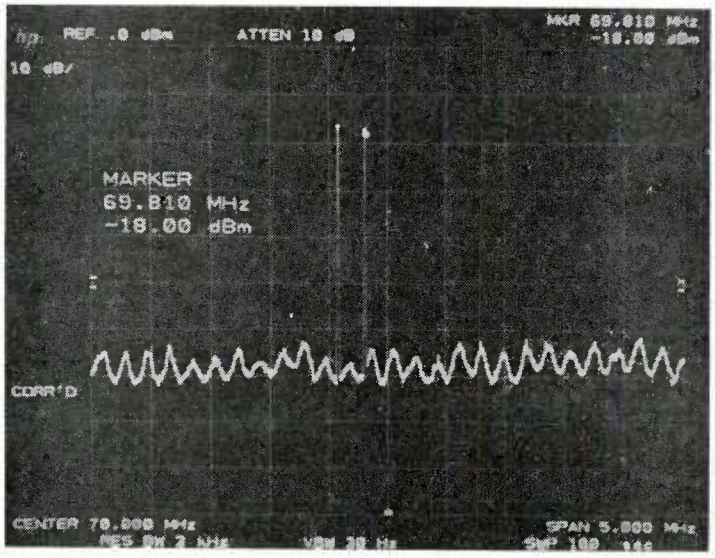

Fig. 9 — Power spectrum of optical detector output showing oscillatory noise floor/frequency response resulting from the far-end reflection from a 500 meter link into the near-end laser cavity.

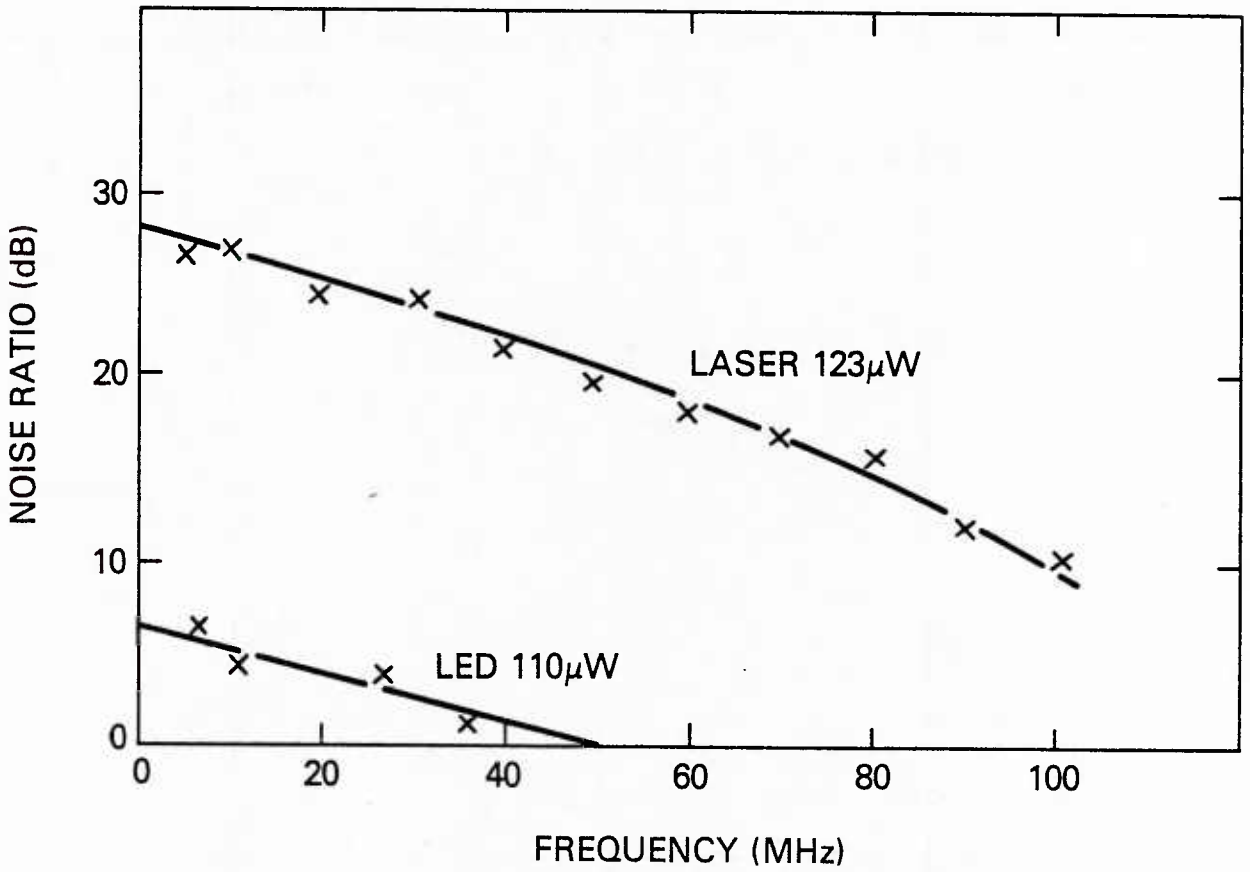

Fig. 10 — Ratio of illuminated/dark receiver noise as a function of frequency for LED and laser illumination.

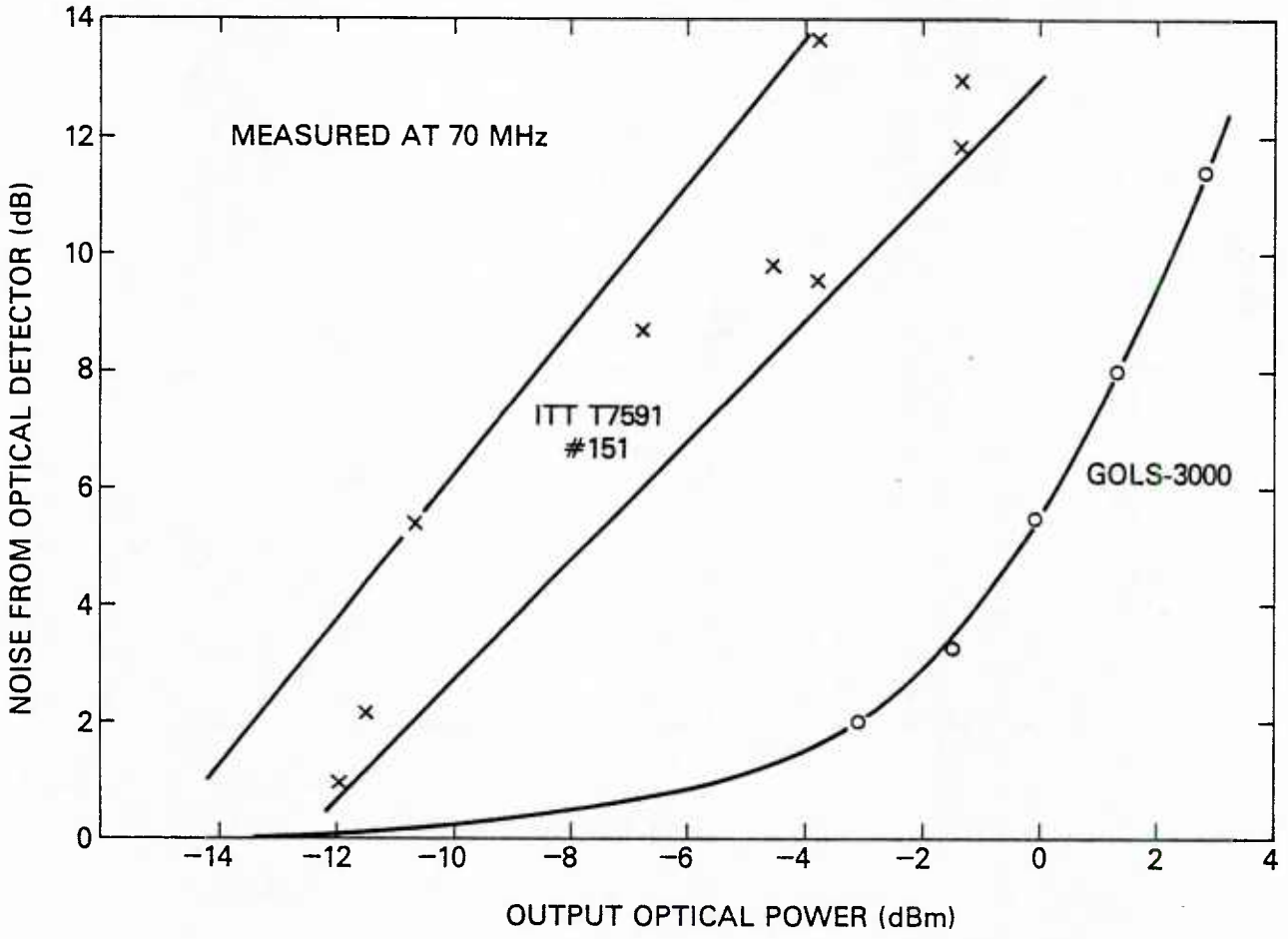

Fig. 11 — Noise comparison of GOLS-3000 and ITT T7591 (#151) lasers as a function of average (output) optical power in decibels relative to 1 mW. Noise reference of 0 dB represents the dark (thermal) noise of the photodetector.

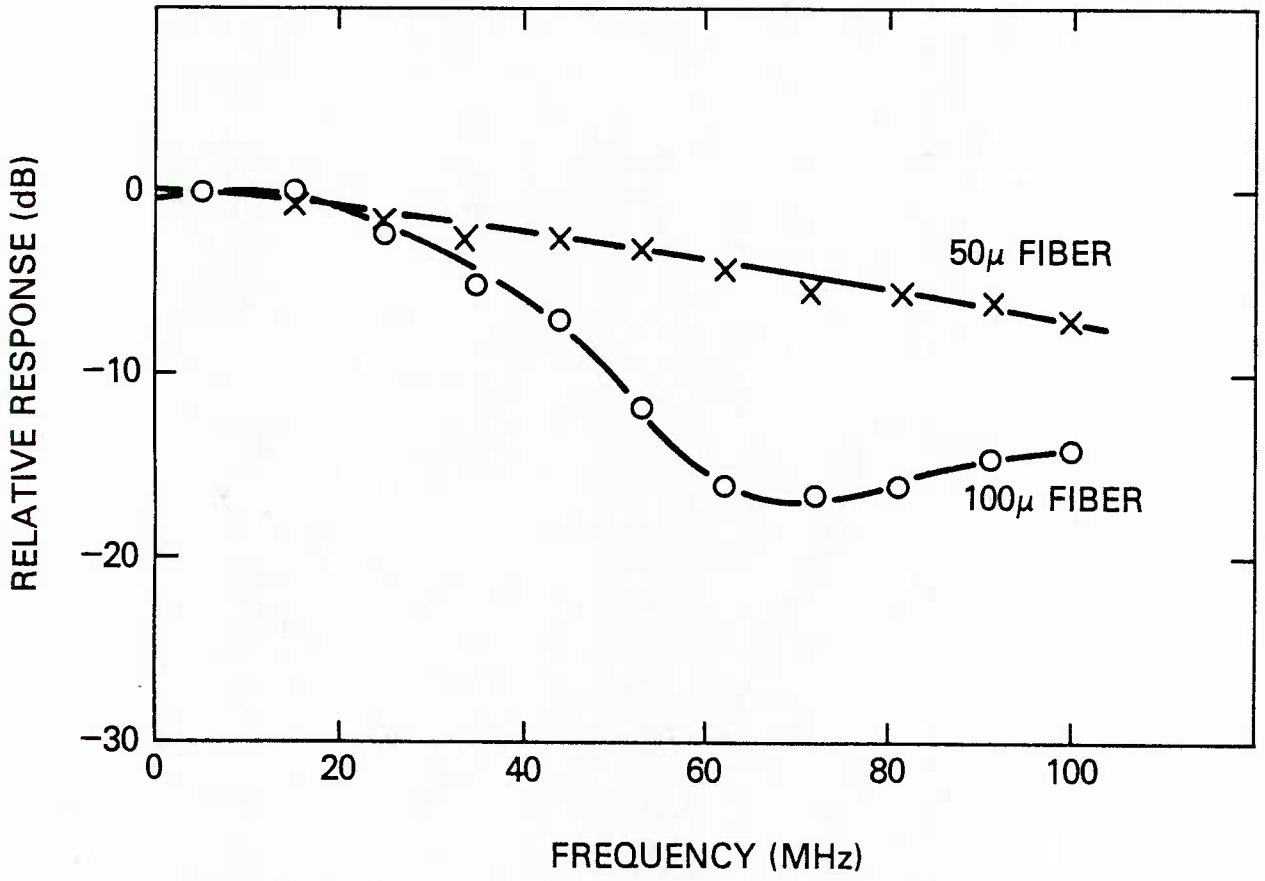

Fig. 12 — Frequency response of Plessey HR810F2 LED with 620 meters of Corning SDF (100 micron core, 25 MHz-km) fiber and 500 meters of ITT graded index (50 micron core) fiber.

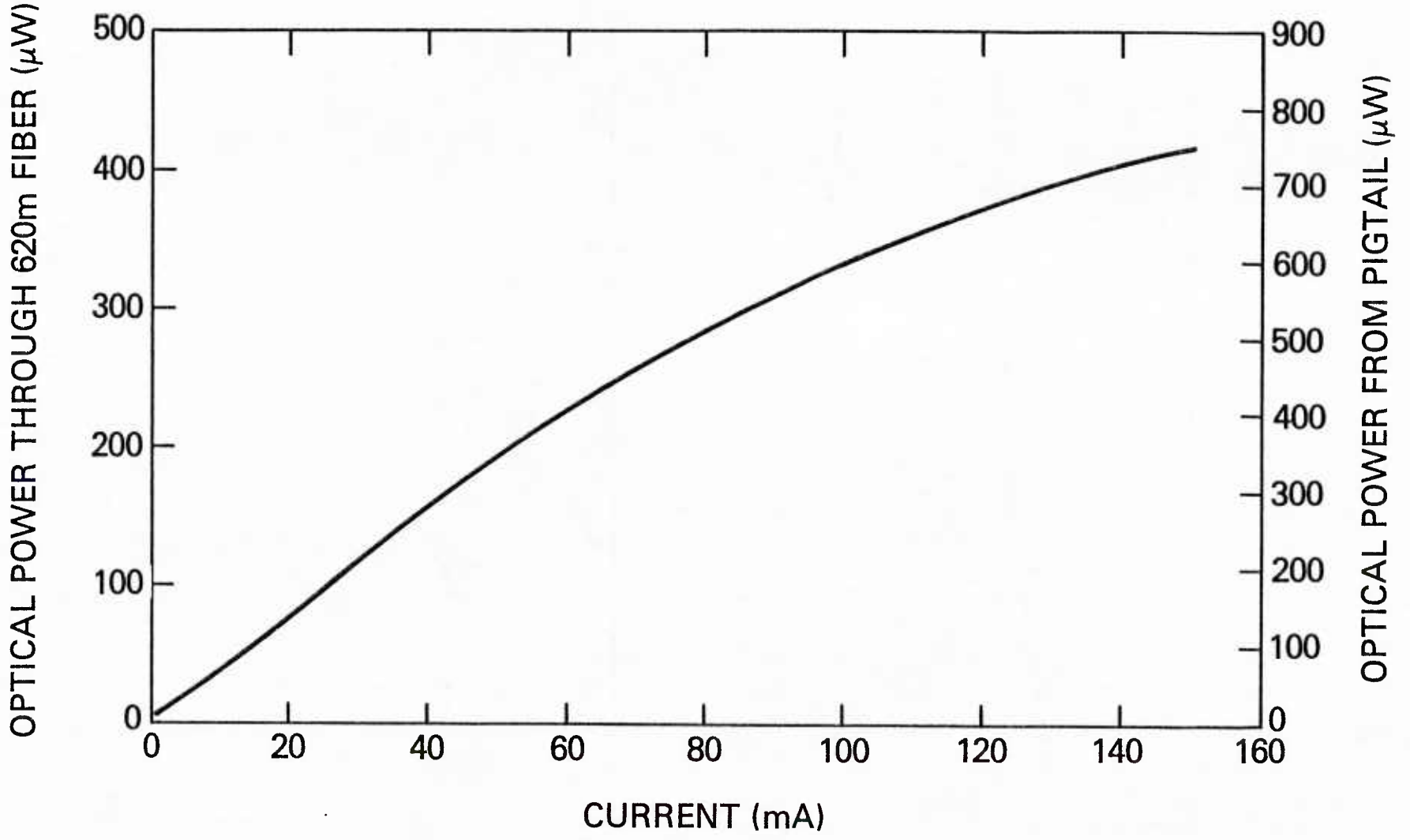

Fig. 13 — Optical transfer characteristic for Plessey HR810F2 (#042) LED.

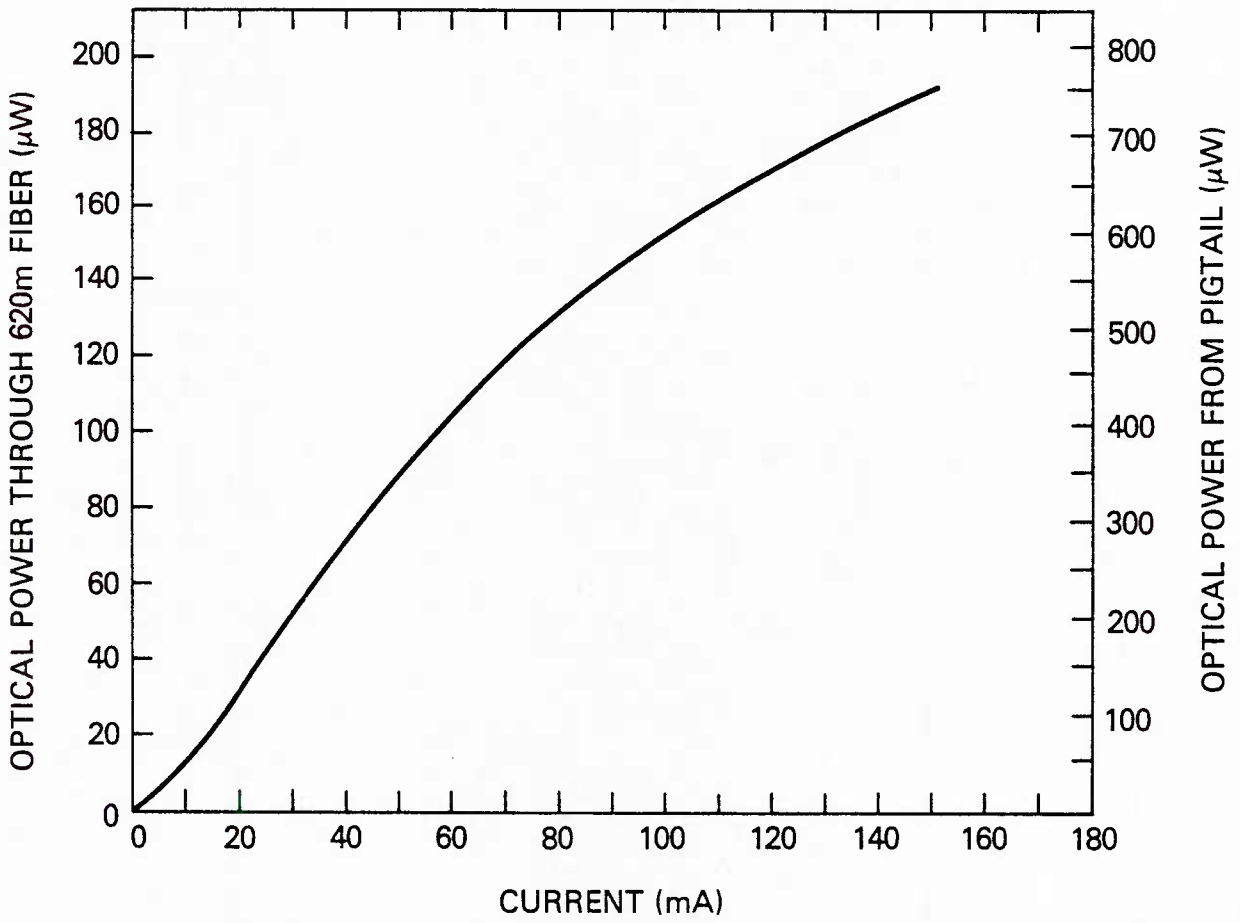

Fig. 14 — Optical transfer characteristic for Plessey HR810F2 (#039) LED.

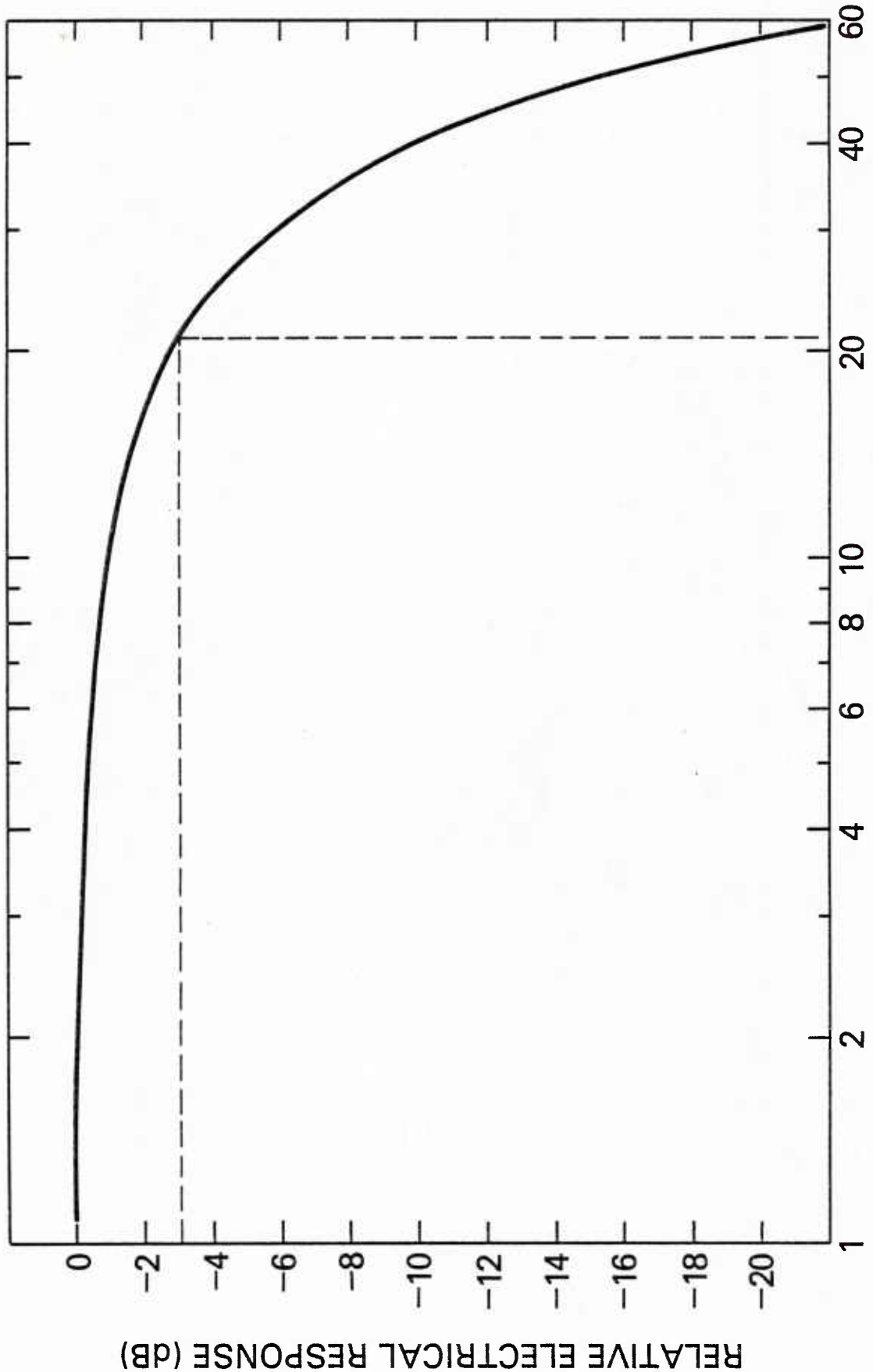

Fig. 15 — Frequency response of Laser Diodes, Inc. IRE-160FA LED with 620 meters of Corning SDF fiber.

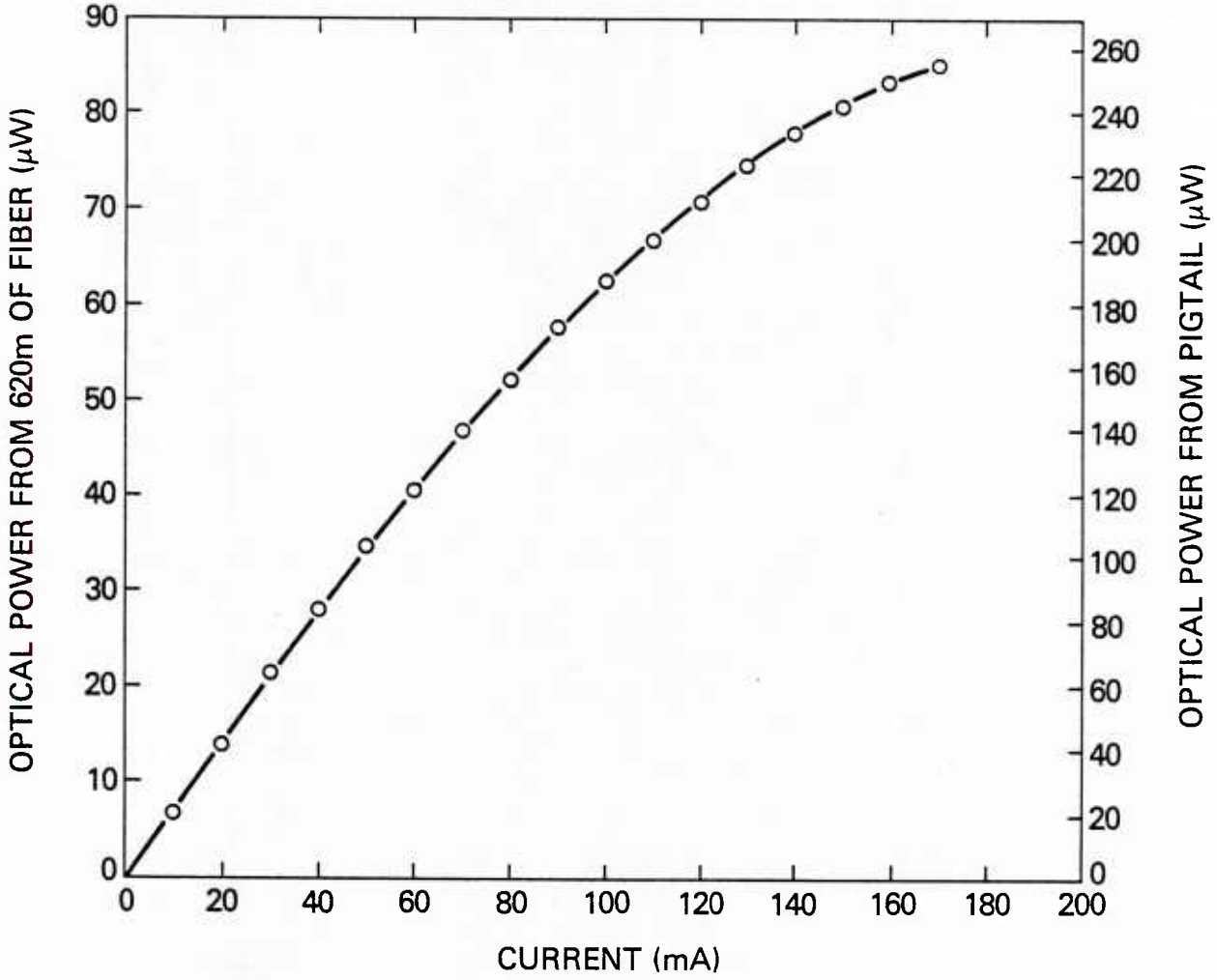

Fig. 16 — Optical transfer characteristic of Laser Diodes, Inc. IRE-160FA LED.

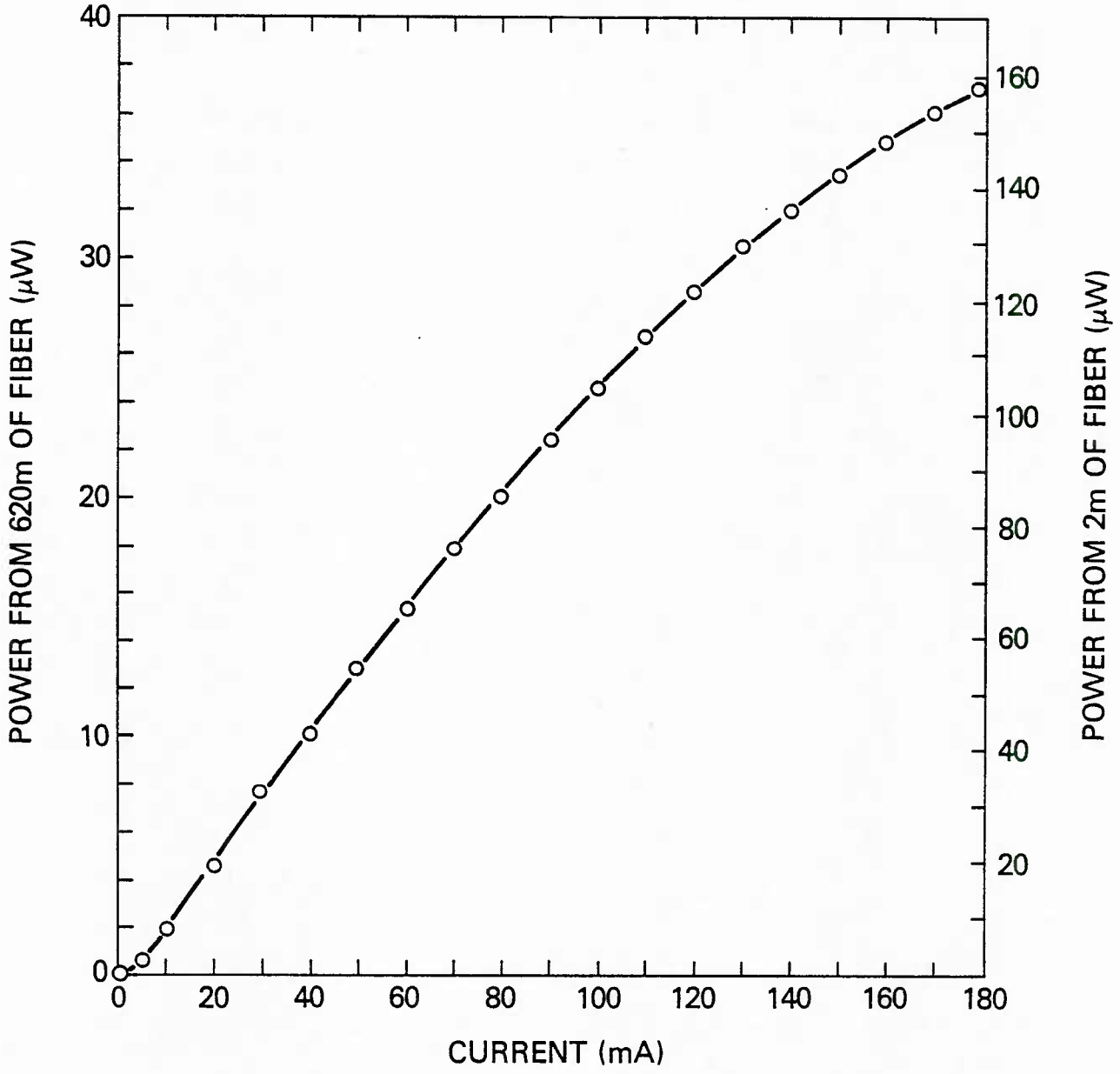

Fig. 17 — Optical transfer characteristic of Motorola MFOE108F LED.

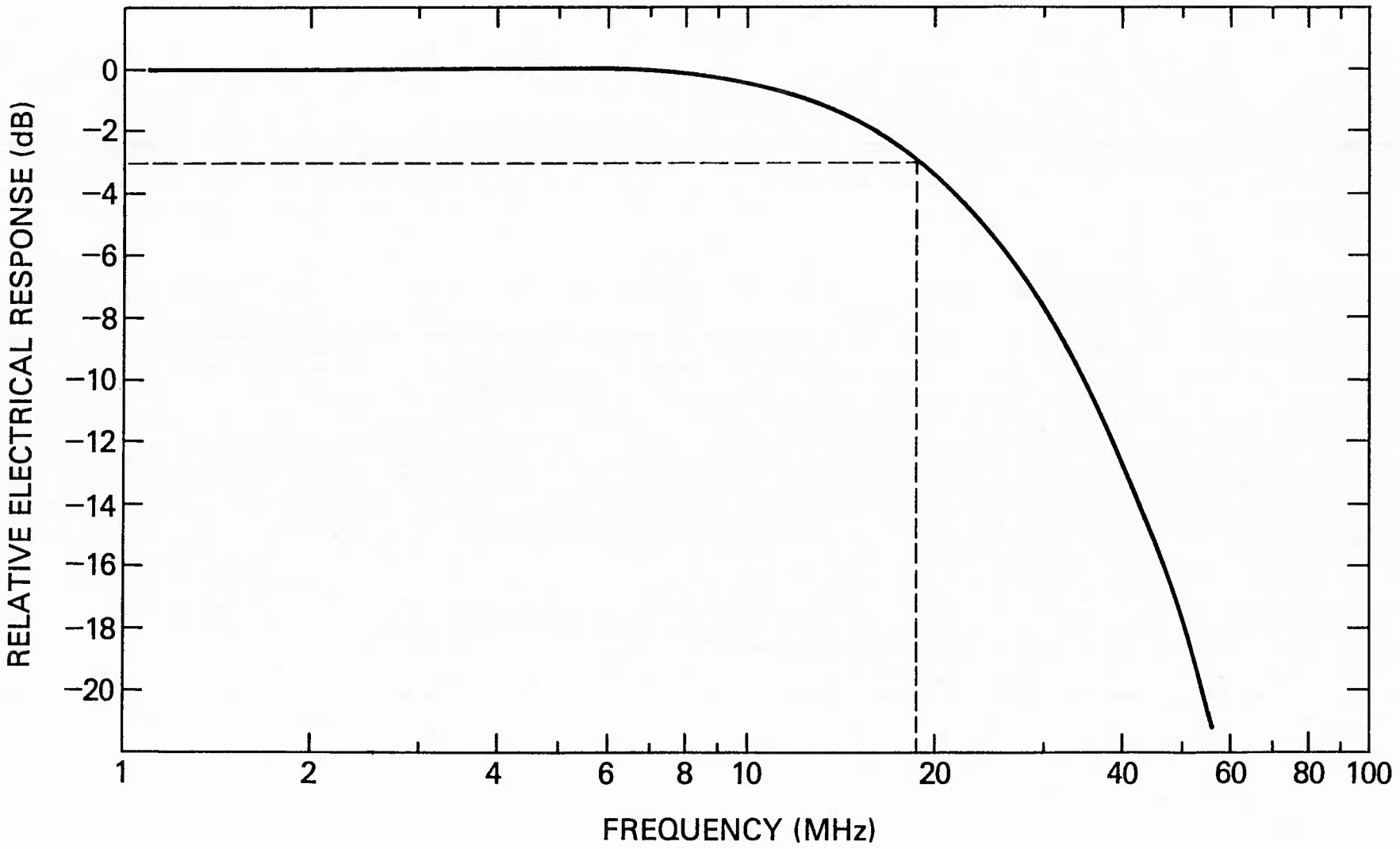

Fig. 18 — Frequency response of Motorola MFOE108F LED with 620 meters of Corning SDF fiber.

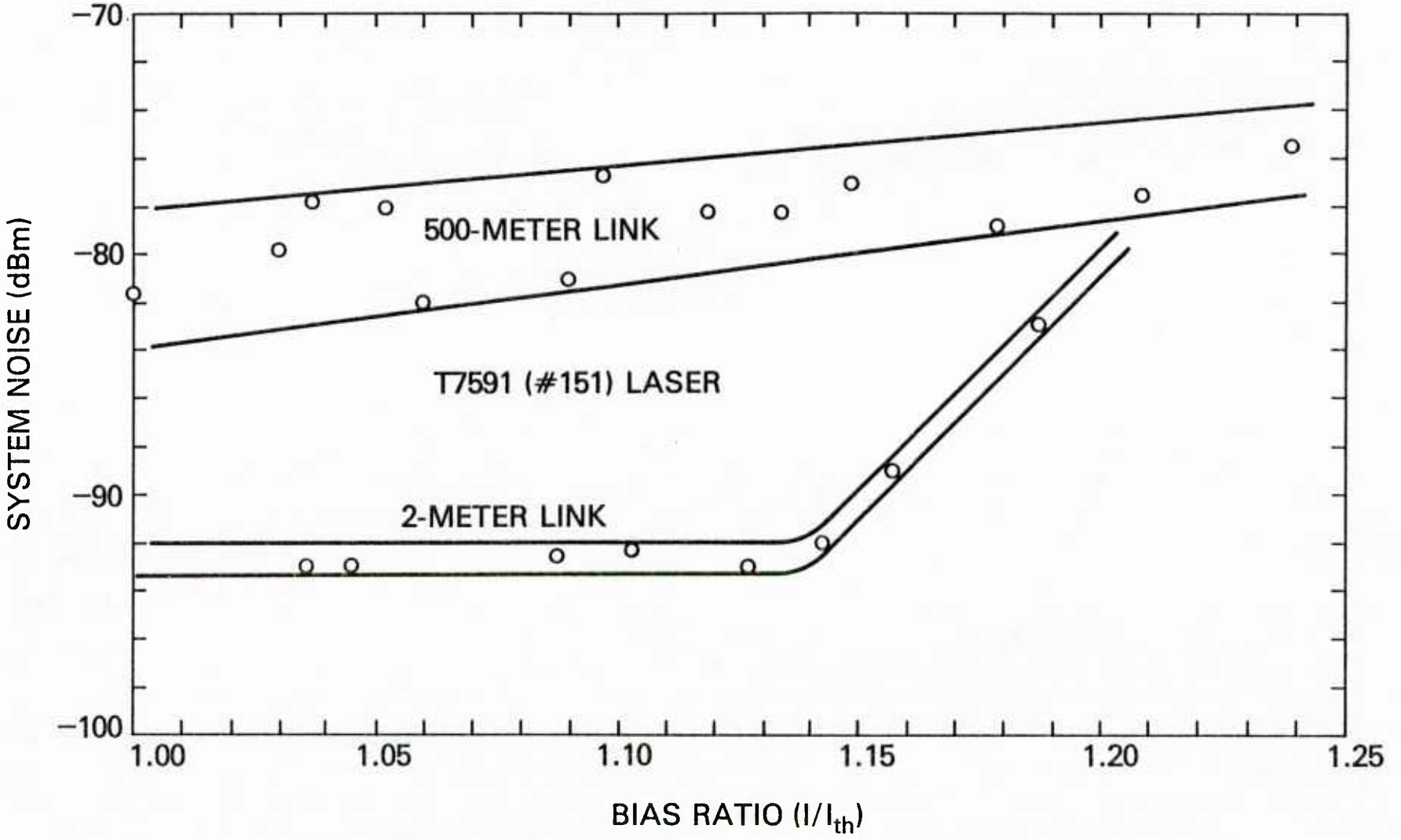

Fig. 19 — Comparison of optical system noise as function of laser I/I_{th} ratio for 2-meter and 500-meter link lengths.

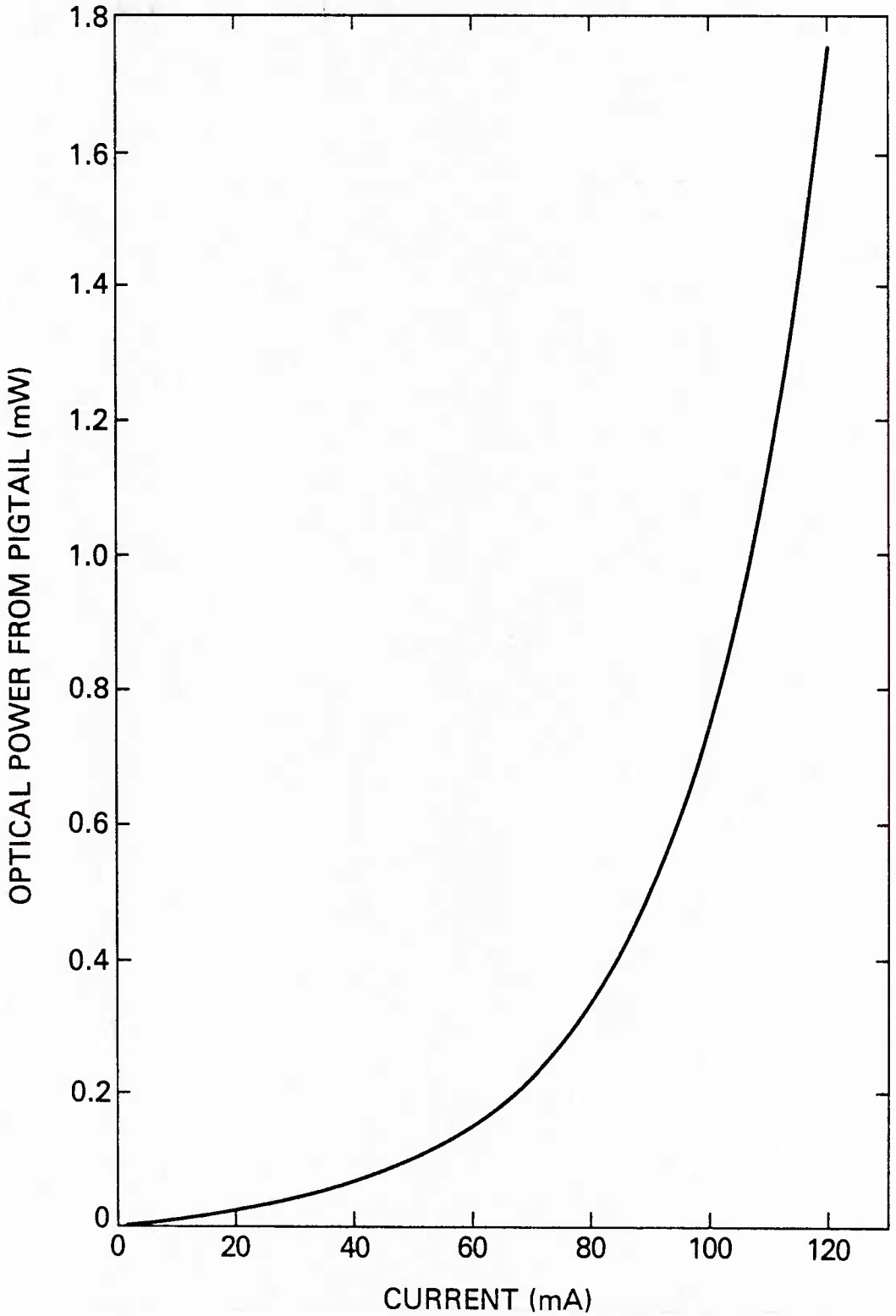

Fig. 20 — Optical transfer characteristic for General Optronics GOLS-3000 super-radiant laser diode.

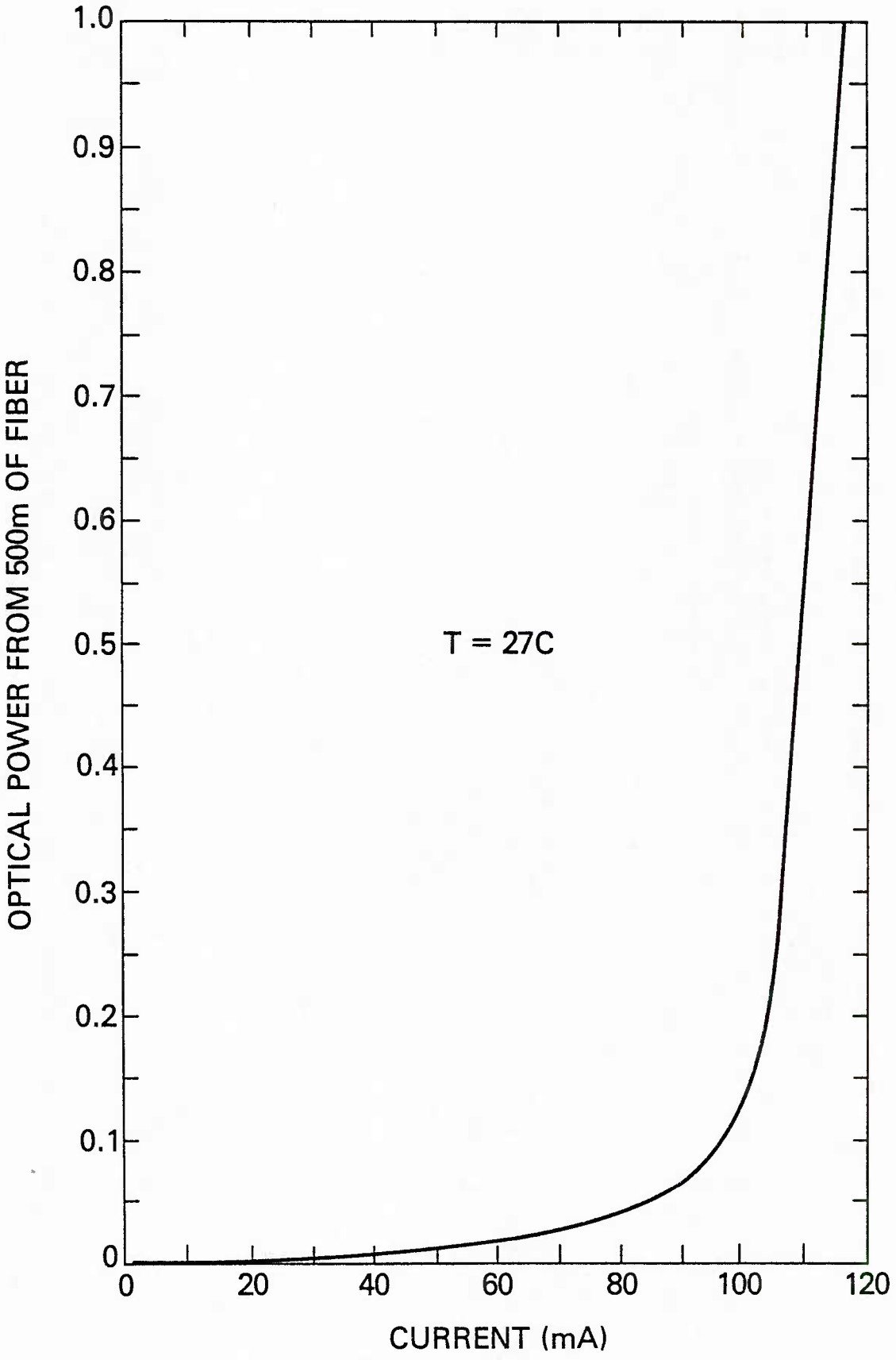

Fig. 21 — Optical transfer characteristic for Laser Diodes, Inc. SCW-20F laser (#225).

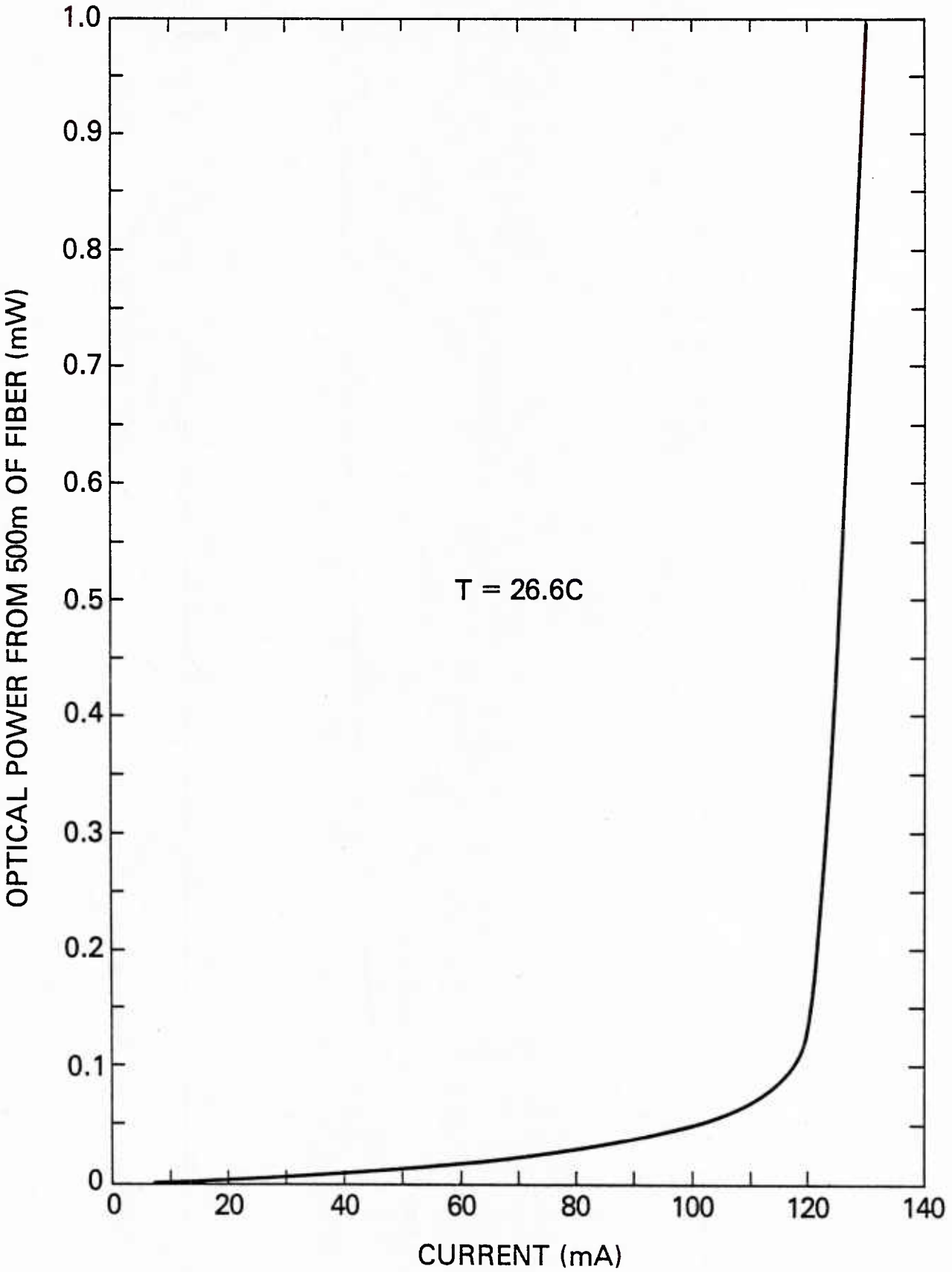

Fig. 22 — Optical transfer characteristic for Laser Diodes, Inc. SCW-20F laser (#131).

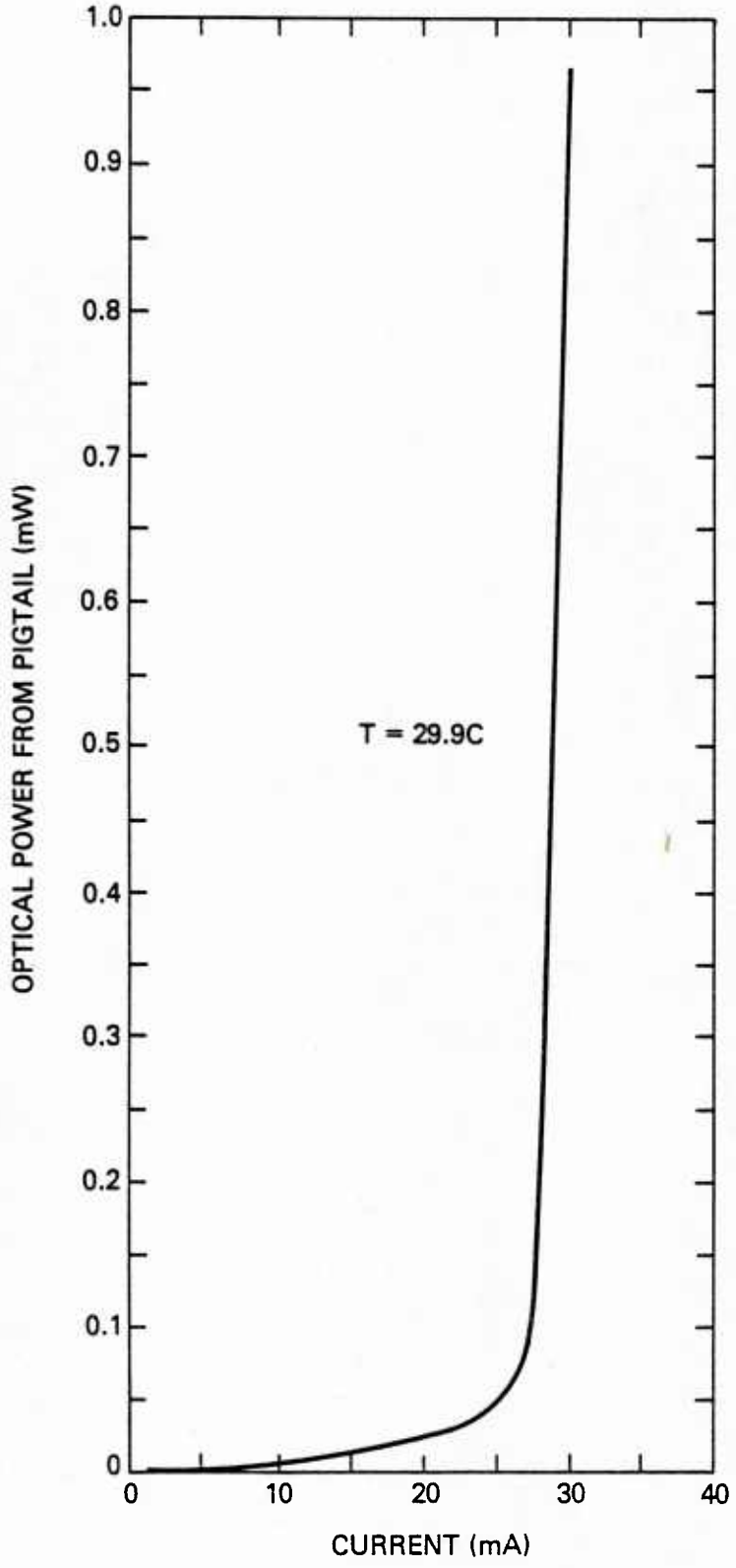

Fig. 23 — Optical transfer characteristic for Laser Diodes, Inc. SCW-20F laser (#133).

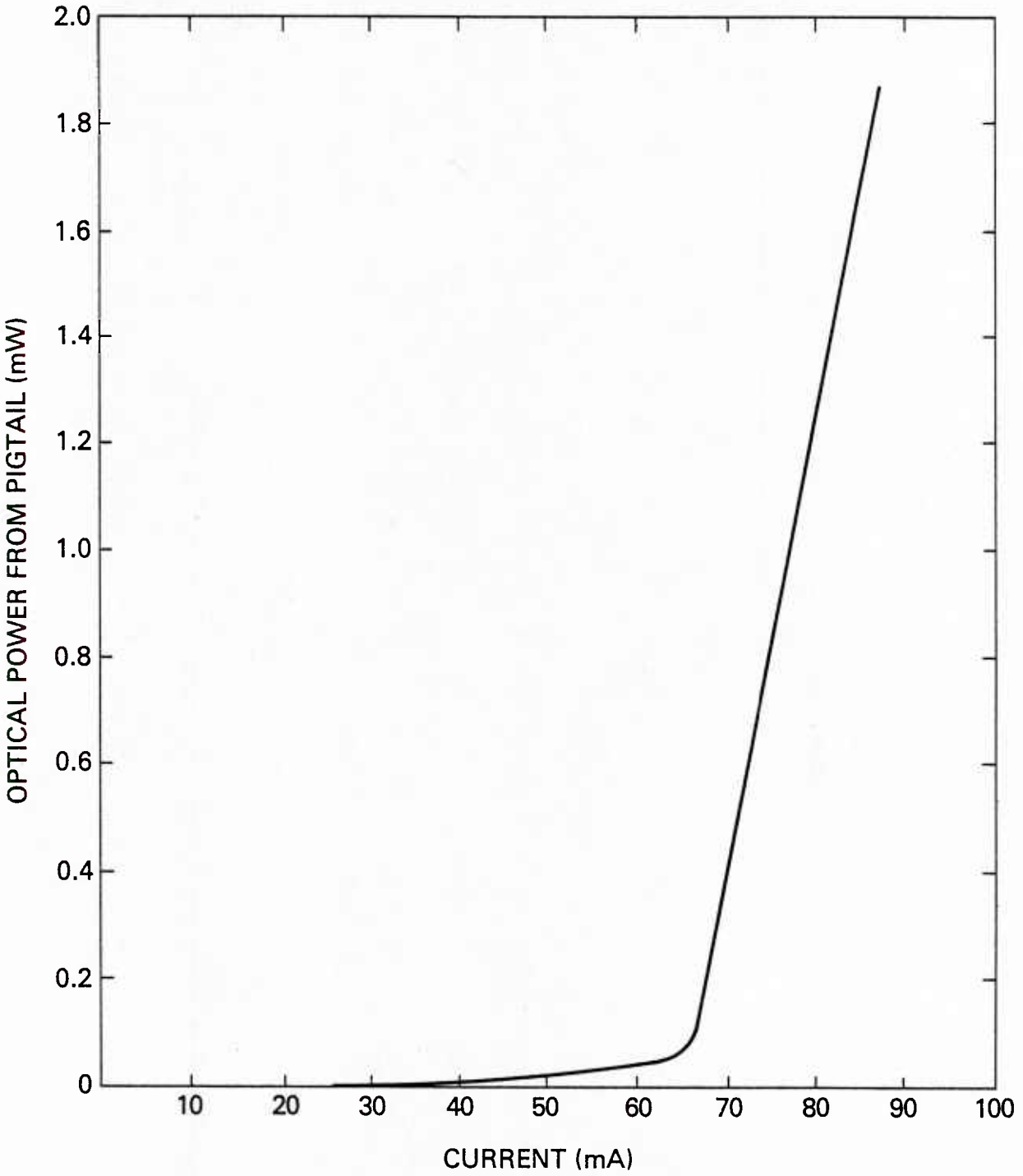

Fig. 24 — Optical transfer characteristic for ITT T7591 laser (#151).

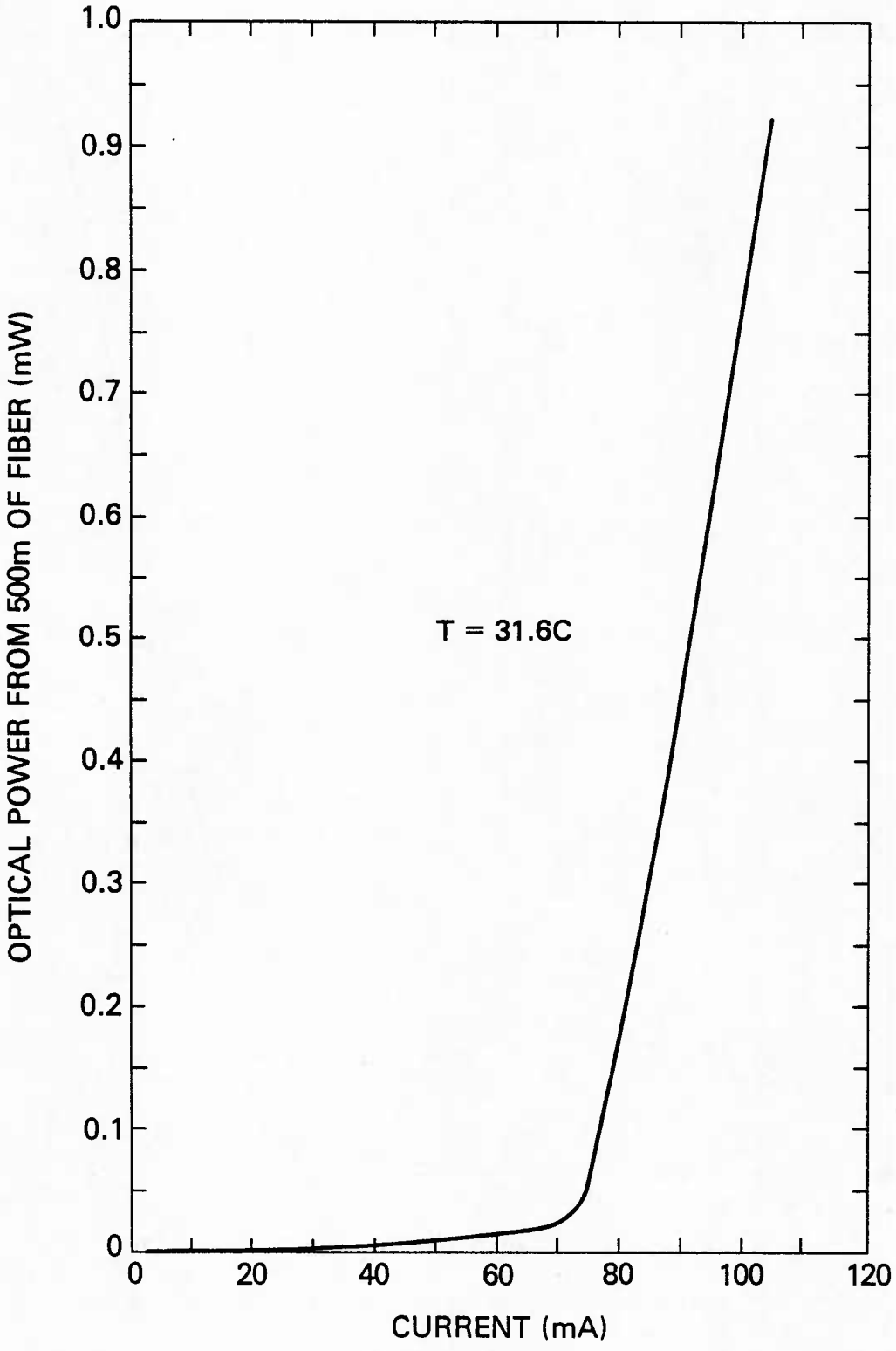

Fig. 25 — Optical transfer characteristic for ITT T7591 laser (#153).

References

1. E. L. Althouse and D. M. Kopp, "Fiber-Optic Transfer of Radio Signals From an Antenna Using an Intermediate FM Carrier," NRL Memorandum Report 5115, July 6, 1983.

2. H. B. Kim and J. Conradi, "A Long Wavelength LED Based Multichannel Video Transmission System Using FM," Sixth European Conference on Optical Communication, pp. 398-401, University of York, United Kingdom, 16-19 September 1980.

3. A. C. Deichmiller, "Progress in Fiber Optics Transmission Systems for Cable Television," IEEE Transactions on Cable Television, Vol. CATV-5, No. 2, pp. 50-59, April 1980.

4. J. R. Fisk, "Receiver Noise Figure, Sensitivity, and Dynamic Range - What the Numbers Mean," Ham Radio Magazine, pp. 8-25, October 1975.

5. Y. L. Mirtich, "Designer's Guide to: Fiber-Optic data links-Part 3," pp. 103-110, EDN, August 20, 1980.

6. M. Grossman, "Focus on fiber-optic connectors: Low-Cost linking still a challenge," Electronic Design, pp. 255-268, November 12, 1981.

7. T. C. Chu and A. R. McCormick, "Measurements of Loss Due to Offset, End Separation and Angular Misalignment in Graded Index Fibers Excited by an Incoherent Source," The Bell System Technical Journal, Vol, 57, No. 3, pp. 595-602, March 1978.

8. P. Keeler, "Alignment is the fiber-optic connector's main job-but accuracy starts with fibers," pp. 104-108, Electronic Design, Vol. 22, October 25, 1978.

9. C. P. Sandbank, Optical Fibre Communication Systems, p. 88, John Wiley and Sons, Ltd, 1980.

10. M. J. Howes and D. V. Morgan, Optical Fibre Communications, p. 298, John Wiley and Sons Ltd, 1979.

11. D. Gloge, "Bending Loss in Multimode Fibers with Graded and Ungraded Core Index," pp. 2506-2513, Applied Optics, Vol. 11, No. 11, November 1972.

12. D. Marcuse, "Microbending Losses of Single-Mode, Step-Index and Multimode, Parabolic-Index, Fibers," pp. 937-955, The Bell System Technical Journal, V. 55, No. 7, 1976.

13. G. A. Wilkins, "Guidelines to the Design of Optical Cables," ASME Publication 79-WA/OCE-6, Presented at the Winter Annual Meeting of the Ocean Engineering Division of the American Society of Mechanical Engineers, New York, NY, December 2-7, 1979.

14. C. M. Miller, Laminated Fiber Ribbon for Optical Communication Cables," pp. 929-935, The Bell System Technical Journal, September 1976.

15. M. D. Rourke and J. A. Wysocki, "Empirical formula for coating-induced excess loss in fiber waveguides," paper Tu F3, Conference Proceedings of 1979 Optical Fiber Communications.

16. R. Olshansky, "Distortion Losses in Cabled Optical Fibers," Applied Optics, Vol. 14, No. 1, pp. 20-21, January 1975.

17. W. B. Gardner, S. R. Nagel, M. I. Schwartz, F. V. Dimarcello, C. R. Lovelace, D. L. Brownlow, M. R. Santana, and E. A. Sigety, "The Effect of Optical Fiber Core and Cladding Diameter on the Loss Added by Packaging and Thermal Cycling," The Bell System Technical Journal, Vol. 60, No. 6, pp. 859-864, July-August 1981.

18. R. E. Epworth, "Phenomenon of Modal Noise in Fiber Systems," Optical Fiber Communications Proceedings, (New York, IEEE) paper Th D1, pp. 106-108. March 1979.

19. R. E. Epworth, "The Phenomenon of Modal Noise in Analogue and Digital Optical Fiber Systems," Proceedings of the 4th European Conference on Optical Communications, Genoa, September 1978.

20. H. Olesen, E. Nicolaisen, and M. Danielsen, "Quantitative Experimental Results on Modal Distortion and Comparison with Theory Based on AM-FM Conversion," Sixth European Conference on Optical Communication, University of York, United Kingdom, pp. 84-87, 16-19 September 1980.

21. E. G. Rawson, J. W. Goodman, and R. E. Norton, "Experimental and Analytical Study of Modal Noise in Optical Fibers," Sixth European Conference on Optical Communication, University of York, United Kingdom, pp. 72-75, 16-19 September 1980.

22. K. Petermann, "Nonlinear Distortions Due To Fibre Connectors," Sixth European Conference on Optical Communication, University of York, United Kingdom, 16-19 September 1980, pp. 80-83.

23. E. G. Rawson, "Modal noise in multimode fibers: polarization effects," paper WS3, Conference On Lasers and Electro-optics, IEEE/OSA, Washington, D.C., 10-12 June 1981, pg. 72.

24. T. P. Lee, "Recent development in light-emitting diodes (LEDs) for optical fiber communication systems," pp. 92-101, SPIE, Vol. 224, Fiber Optics for Communications and Control, 1980.

25. S. D. Personick, "Receiver Design for Digital Fiber Optic Communication Systems, I," Bell System Technical Journal, Vol. 52, pp. 843-874, July-Aug. 1973.

26. S. D. Personick, "Receiver Design for Digital Fiber Optic Communication Systems, II," Bell System Technical Journal, Vol. 52, pp. 875-886, July-Aug. 1973.

27. F. M. E. Sladen and C. M. Look, "Distortion In Semiconductor Lasers and Its Dependence On System Components," Sixth European Conference on Optical Communication, pp 195-198, University of York, United Kingdom, 16-19 September 1980.

28. O. Hirota and Y. Suematsu, "Noise Properties of Injection Lasers Due to Reflected Waves," IEEE Journal of Quantum Electronics, Vol QE-15, No 3, pp. 142-149, March 1979.

29. T. Kanada and K. Nawata, "Injection Laser Characteristics due to Reflected Optical Power," IEEE Journal of Quantum Electronics, Vol. QE-15, No. 7, pp. 559-565, July 1979.

30. M. Ito and T. Kimura, "Longitudinal Mode Competition in a Pulse Modulated AlGaAs DH Semiconductor Laser," IEEE Journal of Quantum Electronics, Vol. QE-15, No. 7, pp. 542-544, July 1979.

31. I. Ito, S. Machida, K. Nawata, and T. Ikegami, "Intensity Fluctuations in Each Longitudinal Mode of a Multimode AlGaAs Laser," IEEE Journal of Quantum Electronics, Vol. QE-13, No. 8, pp. 574-579, August 1977.

32. Y. Okano, K. Nakagawa, and T. Ito, "Laser Mode Partition Noise Evaluation for Optical Fiber Transmission," IEEE Transactions on Communications, Vol. COM-28, No. 2, pp. 238-243, February 1980.

33. G. H. Olsen, D. J. Channin, and M. Ettenberg, "Fiber optical communications: concepts, components and systems," RCA Engineer, 26-3, pp. 42-53, Nov/Dec 1980.

34. J. F. Svacek, "Transmitter feedback techniques stabilize laser-diode output," Electronic Design News (EDN), March 5, 1980.

35. E. L. Althouse and D. M. Kopp, "A Novel Concept for a Remotely Located, Tunable Radio Receiver Using an Analog Fiber-Optic Link," NRL Memorandum Report 4909, September 30, 1982.

U210728

DEPARTMENT OF THE NAVY

NAVAL RESEARCH LABORATORY
Washington, D.C. 20375

OFFICIAL BUSINESS
PENALTY FOR PRIVATE USE, $300

POSTAGE AND FEES PAID
DEPARTMENT OF THE NAVY
DoD-316

THIRD CLASS MAIL